

Dissertation zur Erlangung des Doktorgrades  
der Fakultät für Chemie und Pharmazie  
der Ludwig-Maximilians-Universität München



**Targeting cyclin dependent kinase 5  
in hepatocellular carcinoma**

—

**a novel therapeutic approach**

Sandra Monika Ehrlich

(geb. Stamm)

aus Ebersberg, Deutschland

2014

## **Erklärung**

Diese Dissertation wurde im Sinne von §7 der Promotionsordnung vom 28. November 2011 von Frau Prof. Dr. Angelika M. Vollmar betreut.

## **Eidesstattliche Versicherung**

Diese Dissertation wurde eigenständig und ohne unerlaubte Hilfe erarbeitet.

München, den

---

Sandra Monika Ehrlich

Dissertation eingereicht am:	24.06.2014
1. Gutachter:	Prof. Dr. Angelika M. Vollmar
2. Gutachter:	Prof. Dr. Stefan Zahler
Mündliche Prüfung am:	25.07.2014

*To my family and friends*

# CONTENTS

# CONTENTS

<b>1</b>	<b>INTRODUCTION.....</b>	<b>10</b>
1.1	Hepatocellular carcinoma.....	10
1.2	Cyclin dependent kinase 5 .....	10
1.2.1	Regulation of Cdk5 .....	11
1.2.2	Function of Cdk5 in the nervous system.....	12
1.2.3	Function of Cdk5 in cancer .....	13
1.2.4	Pharmaceutical inhibition of Cdk5 .....	13
1.3	Aim of the study .....	14
<b>2</b>	<b>MATERIALS AND METHODS.....</b>	<b>16</b>
2.1	Materials.....	16
2.1.1	Compounds .....	16
2.1.2	Reagents and technical equipment .....	16
2.2	Cell culture .....	18
2.2.1	Solutions and reagents.....	18
2.2.2	Cell lines .....	19
2.2.3	Passaging.....	19
2.2.4	Freezing and thawing .....	19
2.3	Transfection experiments.....	20
2.3.1	Cdk5 and p27 <sup>Kip1</sup> siRNA .....	20
2.3.2	Cdk5 shRNA.....	20
2.4	Western blot analysis .....	21
2.5	Nuclear/cytoplasmic fractionation.....	23
2.6	Immunoprecipitation.....	24

---

<b>2.7</b>	<b>Kinase activity assay .....</b>	<b>24</b>
<b>2.8</b>	<b>Human HCC microarrays.....</b>	<b>25</b>
<b>2.9</b>	<b>Immunohistochemistry.....</b>	<b>25</b>
2.9.1	Cdk5 and Ki-67 .....	25
2.9.2	Terminal deoxynucleotidyl transferase dUTP nick end labeling (TUNEL) .....	26
<b>2.10</b>	<b>Immunostaining.....</b>	<b>26</b>
<b>2.11</b>	<b>Proliferation assays .....</b>	<b>27</b>
2.11.1	Crystal violet staining.....	27
2.11.2	Impedance measurement.....	27
<b>2.12</b>	<b>Colony formation assay.....</b>	<b>28</b>
<b>2.13</b>	<b>Motility assays.....</b>	<b>28</b>
2.13.1	Boyden Chamber assay .....	28
2.13.2	Wound healing assay .....	28
<b>2.14</b>	<b>Cell cycle and apoptosis analysis .....</b>	<b>29</b>
<b>2.15</b>	<b><i>In vivo</i> assays .....</b>	<b>30</b>
2.15.1	Animals.....	30
2.15.2	Tumor cell implantation.....	31
2.15.3	Intraperitoneal application of roscovitine and irinotecan .....	31
2.15.4	Isolation of tumors .....	31
<b>2.16</b>	<b>Statistical analysis .....</b>	<b>31</b>
<b>3</b>	<b>RESULTS .....</b>	<b>33</b>
<b>3.1</b>	<b>Cdk5 expression is increased in human HCC.....</b>	<b>33</b>
<b>3.2</b>	<b>Abrogation of Cdk5 inhibits HCC progression <i>in vitro</i> and <i>in vivo</i>.....</b>	<b>35</b>

---

3.2.1	Blockage of Cdk5 function inhibits HCC cell growth and motility <i>in vitro</i> .....	35
3.2.2	Inhibition of Cdk5 reduces HCC tumor growth in a xenograft mouse model.....	40
<b>3.3</b>	<b>Function of Cdk5 in the nucleus of HCC cells .....</b>	<b>42</b>
3.3.1	Cdk5 is localized in the nucleus of proliferating HCC cells .....	42
3.3.2	Cdk5 is activated in the nucleus of cells in the G2/M cell cycle phase.....	44
3.3.3	Cdk5 gets activated by DNA damage and is involved in DNA damage response.....	46
3.3.4	Cdk5 influences DNA damage checkpoint regulation.....	48
3.3.5	Cdk5 is important for ATM phosphorylation.....	50
<b>3.4</b>	<b>Cdk5 inhibition chemosensitizes HCC cells for treatment with DNA damage chemotherapeutics .....</b>	<b>52</b>
<b>3.5</b>	<b>Cdk5 inhibition enhances efficacy of sorafenib treatment in HCC cells.....</b>	<b>56</b>
3.5.1	Cdk5 inhibition acts synergistic with sorafenib on HCC tumor growth.....	56
3.5.2	Inhibition of Cdk5 prevents the cell migration induced by low-dose sorafenib .....	57
<b>4</b>	<b>DISCUSSION.....</b>	<b>59</b>
4.1	Cdk5 is an important mediator in HCC progression.....	59
4.2	Cdk5 regulates DNA damage response and checkpoint activation <i>via</i> ATM pathway .....	60
4.3	Combination of Cdk5 inhibition with DNA damage agents presents a novel therapeutic option for HCC .....	62
4.4	Cdk5 inhibition increases efficacy and response to sorafenib treatment.....	63

---

4.5	<b>Cdk5 represents a novel drugable target for HCC therapy .....</b>	<b>64</b>
4.6	<b>Conclusion and further perspectives.....</b>	<b>64</b>
5	<b>SUMMARY.....</b>	<b>66</b>
6	<b>REFERENCES.....</b>	<b>68</b>
7	<b>APPENDIX.....</b>	<b>75</b>
7.1	<b>Abbreviations .....</b>	<b>75</b>
7.2	<b>Publications .....</b>	<b>77</b>
7.2.1	Original publications .....	77
7.2.2	Poster presentations.....	77
7.3	<b>Acknowledgements.....</b>	<b>79</b>

# INTRODUCTION

# 1 INTRODUCTION

## 1.1 Hepatocellular carcinoma

Hepatocellular carcinoma (HCC) is the fifth most common cancer worldwide and the third leading cause of cancer-related death. It accounts for 695,900 deaths per year and its incidence rate is increasing. Chronic liver injuries and cirrhosis caused by hepatitis B or C virus infection, alcoholic liver disease and inherited metabolic diseases contribute most frequently to the development of HCC.<sup>1, 2</sup> Liver transplantation and surgical resection are the major choices of curative treatment for patients with early-stage HCC. Radiofrequency ablation (RFA), transarterial chemoembolization (TACE) and radioembolization are additional therapeutic options for intermediate-stage HCC. Nevertheless in most cases HCC is diagnosed at an advanced stage when these approaches are no longer feasible.<sup>3-5</sup> The only approved systemic therapeutic option for this stage is oral sorafenib treatment.<sup>6</sup> However, the prognosis for these patients is still poor, because the response to sorafenib remains low and the median overall survival is only extended by 2.8 months.<sup>7</sup> Therefore, the development of novel targeted therapies for HCC is of paramount clinical importance.

## 1.2 Cyclin dependent kinase 5

Cyclin dependent kinase 5 (Cdk5) was discovered in the early 1990s<sup>8</sup> and shares 60% structural identity with Cdk1 and Cdk2. Nevertheless Cdk5 is a unique member of the Cdk family with respect to its function and regulation. It is not a classical mediator of cell cycle progression, but it regulates the cytoarchitecture in the central nervous system (CNS) and thereby is important for neuronal development, function and disease. A huge number of studies investigated Cdk5 function in the CNS, but during recent years Cdk5 turned out not to be neuron specific. Some reports also indicate a role of Cdk5 in endothelial, epithelial, immune, and cancer cells.<sup>9, 10</sup>

### 1.2.1 Regulation of Cdk5

Almost the complete knowledge about Cdk5 regulation up to now is gained in neuronal cells. In neurons, Cdk5 activity is mainly regulated by association with one of the two obligate Cdk5-specific activator proteins, p35 or p39. Both share about 57% amino acid homology.<sup>9, 11-13</sup> Interestingly, p35 can mask the absence of p39, whereas p39 can compensate only some function of p35.<sup>9, 14</sup>

These two activator proteins themselves are regulated by transcription and ubiquitin-mediated degradation. In addition to the activation, p35/p39 determined the subcellular distribution of Cdk5, as a myristoylation motif targets them to cell membranes and cell periphery.<sup>11, 15</sup> The activity of Cdk5 is reported to be also increased by phosphorylation at Tyr15. The responsible kinases are c-Abelson (c-Abl)<sup>16</sup> and Fyn<sup>17</sup> (Figure 1). However, the influence of this phosphorylation on Cdk5 activity is controversially discussed as Kobayashi *et al.* recently showed in neuronal cells that it has no activating effect on Cdk5.<sup>18</sup>

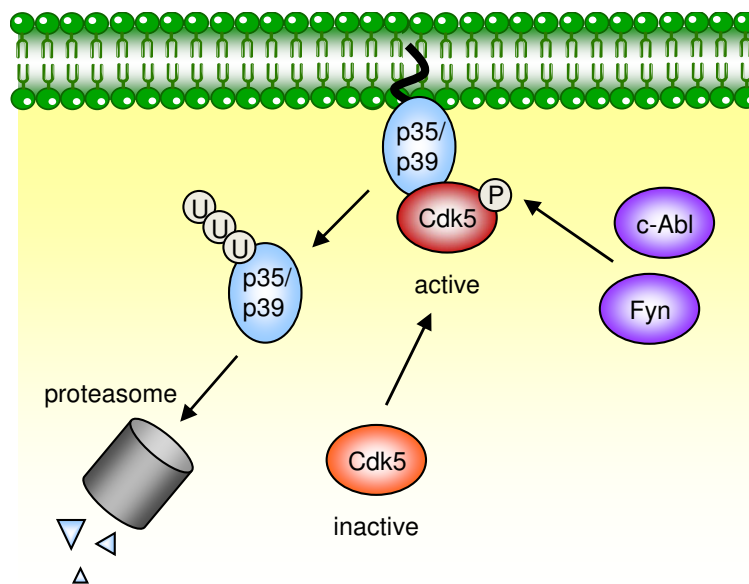


**Figure 1** Regulation of Cdk5. Cdk5 is activated by association with p35 or p39 and *via* phosphorylation at Tyr15 by e.g. c-Abl and Fyn. P35 and p39 are myristoylated and thus recruit Cdk5 by interaction to the cell membrane. Moreover, these activator proteins are regulated by ubiquitin-mediated degradation.

### 1.2.2 Function of Cdk5 in the nervous system

Although Cdk5 is ubiquitously expressed, Cdk5 function is most prominent in cells of neuronal origin. Mice with homozygous deletion of the Cdk5 gene or of both activators, p35 and p39, die perinatally and show a remarkable inversion of the six layers in the cerebral cortex. This is due to a global abnormality of neuronal migration.<sup>19-21</sup> Besides its role in neuronal migration, Cdk5 is also indispensable for axon guidance and synaptic transmission. Thereby, Cdk5 controls learning and memory, and mediates drug addiction, such as the addictive response to cocaine.<sup>9, 10, 22, 23</sup>

Of note, Cdk5 is also involved in the pathogenesis of neurodegenerative diseases. Binding of Cdk5 to the truncated forms of its activators (p25/p29) leads to miss-localized activation of Cdk5 as p25 and p29 lacking the myristoylation motif. This dysregulation of Cdk5 function causes an aberrant target phosphorylation and is involved in the mechanisms of neurodegenerative diseases, including Alzheimer's and Parkinson's disease (Figure 2).<sup>9, 24-27</sup>

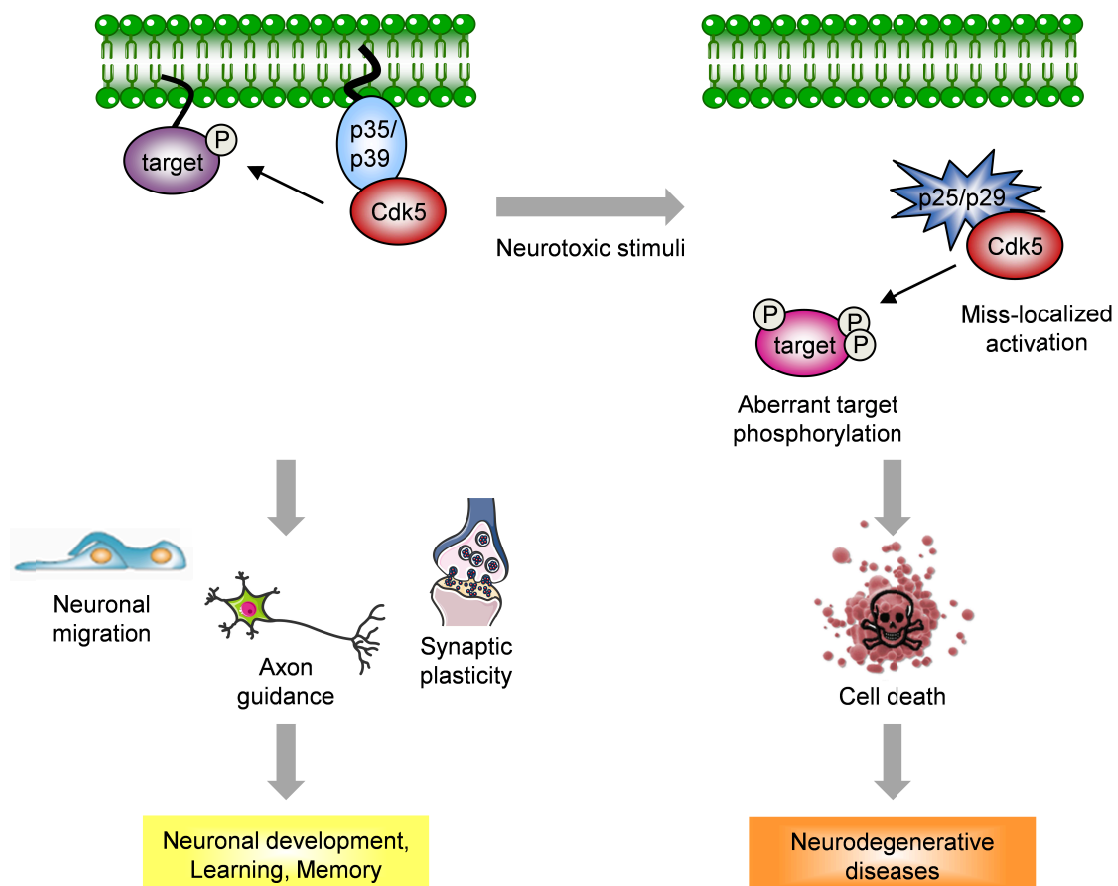


**Figure 2** Overview of Cdk5's function in neurons. Adapted from Liebl *et al.*<sup>10</sup>.

### 1.2.3 Function of Cdk5 in cancer

Over the past decade, the compendium of extraneuronal functions of Cdk5 has expanded.<sup>10, 28, 29</sup> Some publications suggested an association between Cdk5 and human cancer progression. Cdk5 has been implicated in the regulation of prostate cancer cell motility, proliferation of medullary thyroid carcinoma cells, and control of apoptosis in leukemia and astrocytoma cells.<sup>30-36</sup> In pancreatic cancer Cdk5 activity is important for cancer formation, progression and systemic metastasis.<sup>37</sup> Nevertheless, Cdk5's function in cancer is still insufficiently studied and nothing is known about its role in HCC.

### 1.2.4 Pharmaceutical inhibition of Cdk5

The first more or less specific Cdk5 inhibitors were olomoucine<sup>38</sup> and roscovitine (Seliciclib, CYC202).<sup>39</sup> Both compounds belong to the family of 2, 6, 9-trisubstituted purines (Figure 3) and interact with the ATP-binding pocket of the kinases. As this catalytic site is quite conserved throughout the Cdk family, it is hard to design selective inhibitors for one specific Cdk.<sup>40, 41</sup> Various targets of these agents have been identified. Olomoucine inhibits mainly Cdk1, Cdk2, Cdk5 and ERK1,<sup>38, 41</sup> whereas roscovitine targets Cdk1, Cdk2, Cdk5, Cdk7, Cdk9, ERK1/2 and pyridoxal kinase.<sup>39, 40</sup> This pretended disadvantage can be turned into an advantage in context of clinical use, as at least the tumor progression is a multi-factorial disease and multi-target therapeutics might be favored.<sup>42, 43</sup>

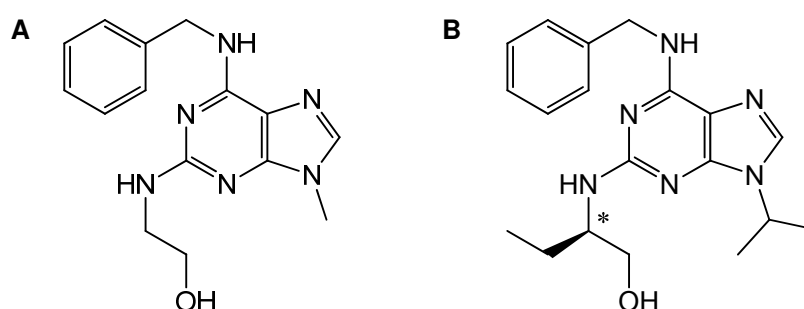


**Figure 3** Chemical structure of (A) olomoucine and (B) (R)-roscovitine.

In context of neurodegenerative diseases some companies are also developing new Cdk5 inhibitors with increased specificity.<sup>44, 45</sup>

### 1.3 Aim of the study

Development of novel efficient therapy for HCC is of paramount clinical importance, as the prognosis for patients with advanced HCC is still very poor. Few reports show an involvement of Cdk5 in tumor progression of e.g. prostate and pancreatic cancer. However, the knowledge on Cdk5's function in cancer is still incomplete and its role in HCC is completely unknown up to now.

Therefore the aim of this study was to investigate the function of Cdk5 in HCC progression, focusing on the major hallmarks: tumor cell motility and tumor cell growth. In addition, the underlying mechanism of Cdk5's influence in HCC cells was examined. Furthermore, novel therapeutic strategies for HCC should be evaluated by combining Cdk5 inhibition with established chemotherapeutics.

## **MATERIALS AND METHODS**

## 2 MATERIALS AND METHODS

### 2.1 Materials

#### 2.1.1 Compounds

(*R*)-Roscovitine, aphidicolin, doxorubicin, etoposide and nocodazol were obtained from Sigma-Aldrich. Sn38 was obtained from Tocris Bioscience. ABT-888 and sorafenib were obtained from Enzo Life Sciences.

#### 2.1.2 Reagents and technical equipment

**Table 1** Biochemicals, inhibitors, dyes and cell culture reagents

Reagent	Producer
32P- $\gamma$ -ATP	Hartmann Analytic, Braunschweig, Germany
AEC substrate	Vector Laboratories, Burlingame, CA, USA
ApopTag <sup>®</sup> Plus Fluorescein <i>In Situ</i> Apoptosis Detection Kit (S7111)	Chemicon International, Atlanta, GA, USA
Bovine serum albumin (BSA)	Sigma-Aldrich, Taufkirchen, Germany
Bradford Reagent <sup>™</sup>	Bio-Rad, Munich, Germany
Collagen G	Biochrom AG, Berlin, Germany
Complete <sup>®</sup>	Roche diagnostics, Penzberg, Germany
Dulbecco's Modified Eagle Medium (DMEM)	PAA Laboratories, Pasching, Austria
DMSO	Sigma-Aldrich, Taufkirchen, Germany
DharmaFECT Transfection reagent	Thermo Scientific, Waltham, MA, USA
FCS	Biochrom AG, Berlin, Germany
FluorSave <sup>™</sup> Reagent	Merck, Darmstadt, Germany
Mayer's Hematoxylin Solution	Sigma-Aldrich, Taufkirchen, Germany
Histone H1 (Type III from calf thymus)	Sigma-Aldrich, Taufkirchen, Germany
Hoechst 33342	Sigma-Aldrich, Taufkirchen, Germany
ibiTreat $\mu$ -slides	ibidi GmbH, Munich, Germany

Reagent	Producer
Matrigel <sup>®</sup>	BD Biosciences, Bedford, MA, USA
Nitrocellulose membrane	Hybond-ECL <sup>™</sup> , Amersham Bioscience, Freiburg, Germany
Nucleofector <sup>™</sup> Kit T	Lonza, Basel, Switzerland
Sodium fluoride (NaF)	Merck, Darmstadt, Germany
Sodium orthovanadate (Na <sub>3</sub> VO <sub>4</sub> )	ICN Biomedicals, Aurora, Ohio, USA
Page Ruler <sup>™</sup> Prestained Protein Ladder	Fermentas, St. Leon-Rot, Germany
Penicillin	PAA Laboratories, Pasching, Austria
Phenylmethylsulfonylfluoride (PMSF)	Sigma Aldrich, Munich, Germany
Propidium iodide	Sigma-Aldrich, Taufkirchen, Germany
Protein G agarose beads	Sigma-Aldrich, Taufkirchen, Germany
RPMI 1640	PAA Laboratories, Pasching, Austria
Streptomycin	PAA Laboratories, Pasching, Austria
Triton X-100	Merck, Darmstadt, Germany
Transwell Permeable Supports (8 μm pore polycarbonate inserts)	Corning Incorporated, New York, NY, USA
Vectastain <sup>®</sup> Universal Elite ABC Kit	Vector Laboratories, Burlingame, CA, USA
X-ray film (Super RX)	Fuji, Düsseldorf, Germany

**Table 2** Technical equipment

Name	Producer
Axioskop microscope	Zeiss, Jena, Germany
Axiovert 25 / 200 microscope	Zeiss, Jena, Germany
Canon 450D camera	Canon, Krefeld, Germany
Canon DS 126181 camera	Canon, Krefeld, Germany
Curix 60	Agfa, Cologne, Germany
FACSCalibur	Becton Dickinson, Heidelberg, Germany
Mikro 22R centrifuge	Hettich, Tuttlingen, Germany
Nucleofector <sup>™</sup> II	Amixa, Cologne, Germany
Olympus DP25 camera	Olympus, Hamburg, Germany
Olympus BX41 microscope	Olympus, Hamburg, Germany

Name	Producer
Odyssey 2.1	LI-COR Biosciences, Lincoln, NE, USA
SpectraFluor Plus™	Tecan, Crailsheim, Germany
Vi-Cell™ XR	Beckman Coulter, Fullerton, CA, USA
xCELLigence System	Roche Diagnostics, Mannheim, Germany
Zeiss LSM 510 Meta confocal laser scanning microscope	Zeiss, Jena, Germany

## 2.2 Cell culture

### 2.2.1 Solutions and reagents

The following solutions and reagents were used for the cultivation of HCC cells.

**Table 3** Solutions and reagents for cell culture

PBS (pH 7.4)		PBS+Ca <sup>2+</sup> /Mg <sup>2+</sup> (pH 7.4)	
NaCl	132.2 mM	NaCl	137 mM
Na <sub>2</sub> HPO <sub>4</sub>	10.4 mM	KCl	2.68 mM
KH <sub>2</sub> PO <sub>4</sub>	3.2 mM	Na <sub>2</sub> HPO <sub>4</sub>	8.10 mM
H <sub>2</sub> O		KH <sub>2</sub> PO <sub>4</sub>	1.47 mM
		MgCl <sub>2</sub>	0.25 mM
		H <sub>2</sub> O	
Growth medium		Freezing medium	
DMEM	500 ml	DMEM	70%
FCSgold (not heat-inactivated)	50 ml	FCSgold (not heat-inactivated)	20%
		DMSO	10%
Trypsin/EDTA (T/E)		Collagen G	
Trypsin	0.05%	Collagen G	0.001%
EDTA	0.20%	PBS	
PBS			

### 2.2.2 Cell lines

HUH7 and HepG2 cells were obtained from Japanese Collection of Research Bioresources (JCRB) and German Research Centre of Biological Material (DSMZ) (ACC180), respectively. All cells were grown in DMEM supplemented with 10% fetal calf serum (FCS). Cells were cultured under constant humidity at 37°C and with 5% CO<sub>2</sub> in an incubator. All culture flasks, multiwell-plates and dishes were first coated with collagen G (0.001% in PBS) before seeding the cells.

### 2.2.3 Passaging

After reaching confluency, cells were either sub-cultured 1:2 - 1:10 in 75 cm<sup>2</sup> culture flasks or seeded either in multiwell-plates or dishes for experiments. For passaging, medium was removed and cells were washed with PBS before incubation with trypsin/ethylene diamine tetraacetic acid (EDTA) (T/E) for 1-2 min at 37°C. Thereafter, cells were gradually detached and the digestion was stopped using growth medium. After adjusting the cell concentration in growth medium and cells were plated.

### 2.2.4 Freezing and thawing

For freezing, confluent cells from a 150 cm<sup>2</sup> flask were trypsinized, centrifuged (1,000 rpm, 5 min, 20°C) and resuspended in ice-cold freezing medium. 1.5 ml aliquots were frozen in cryovials. After storage at -80°C for 24 h, aliquots were moved to liquid nitrogen for long term storage.

For thawing, a cryovial was warmed to 37°C and the content was immediately dissolved in prewarmed growth medium. In order to remove DMSO, cells were centrifuged, resuspended in fresh growth medium and plated in a 25 cm<sup>2</sup> culture flask. The next day cells were washed carefully and after reaching about 80% confluency transferred to a 75 cm<sup>2</sup> culture flask.

## 2.3 Transfection experiments

### 2.3.1 Cdk5 and p27<sup>Kip1</sup> siRNA

Cells were transfected for 24 h to 7 d by lipofection using DharmaFECT Transfection reagent or by electroporation using Nucleofector™II according to the manufacturer's protocol. For Cdk5 silencing two different ON-TARGETplus Cdk5 siRNA were used in an equal mixture (J-003239-09 and J-003239-10; Thermo Scientific). Furthermore, ON-TARGETplus CDKN1B siRNA SMARTpool (L-003472-00; Thermo Scientific) was used for p27<sup>Kip1</sup> silencing and ON-TARGETplus Non-targeting (nt) siRNA (D-001810-01; Thermo Scientific) served as transfection control. Silencing efficiency was examined by Western blot analysis.

### 2.3.2 Cdk5 shRNA

For the lentiviral transduction of HUH7 cells with Cdk5 shRNA and nt shRNA Cdk5 MISSION® shRNA Lentiviral Transduction Particles (Vector: pLKO.1-puro; SHCLNV-NM\_004935; Clone ID: (1) TRCN0000021465, (2) TRCN0000021466, (3) TRCN0000021467, (4) TRCN0000194974, (5) TRCN0000195513; Sigma-Aldrich) and MISSION® pLKO.1-puro Non-Mammalian shRNA Control Transduction Particles (SHC002V; Sigma-Aldrich) as a control were used according to the manufacturer's protocol. HUH7 cells were transduced with a multiplicity of infection (MOI) of one. Successfully transduced cells were selected by adding 2 µg/mL puromycin to the medium. After selection, the concentration of puromycin was reduced to 1 µg/mL for subsequent cultivation of the cells. By this the stable transfection of HUH7 cells with Cdk5 or nt shRNA could be ensured. Cdk5 knockdown of the different shRNA clones was examined by Western blot analysis and most efficient clone number 1 and 4 were used for further experiments.

## 2.4 Western blot analysis

Cells were washed once with ice-cold PBS, lysis buffer was added and cells were frozen at  $-80^{\circ}\text{C}$ . Afterwards, cells were scraped off and debris was removed by centrifugation (14,000 rpm, 10 min,  $4^{\circ}\text{C}$ ). In order to employ equal amounts of protein in all samples for Western blot analysis, protein concentrations were determined using the Bradford assay. After measurement, protein concentration was adjusted by adding SDS sample buffer and samples were heated at  $95^{\circ}\text{C}$  for 5 min. Proteins were separated by SDS-PAGE and transferred to nitrocellulose membranes by electro tank blotting. The membrane was blocked in 5% non-fat dry milk powder (Blotto) for 2h. Antibody incubation was done overnight at  $4^{\circ}\text{C}$ . Secondary antibodies were HRP-coupled or conjugated with an IR-fluorescent Reagent. Chemiluminescence was detected with ECL substrate and exposure to X-ray films or fluorescence was detected with LI-COR Biosciences Odyssey<sup>®</sup>.

**Table 4** Solutions and reagents for Western blot analysis

<b>Lysis buffer</b>		<b>5x SDS sample buffer</b>	
Tris/HCl	50 mM	Tris/HCl pH 6.8	3.125 M
NaCl	150 mM	Glycerol	50%
Nonidet NP-40	1%	SDS	5%
Sodium deoxycholate	0.25%	DTT	2%
SDS	0.10%	Pryonin Y	0.025%
activated $\text{Na}_2\text{VO}_4$	300 $\mu\text{M}$	$\text{H}_2\text{O}$	
NaF	1 mM		
$\beta$ -glycerophosphate	3 mM		
pyrophosphate	10 mM		
$\text{H}_2\text{O}$			
add before use:			
Complete <sup>®</sup> EDTAfree	4 mM		
PMSF	1 mM		
$\text{H}_2\text{O}_2$	600 $\mu\text{M}$		

**Separation gel 7.5%/10%/12%/15%**

Rotiphorese™ Gel 30	25%/33%/40%/50%
Tris (pH 8.8)	375 mM
SDS	0.1%
TEMED	0.1%
APS	0.05%
H <sub>2</sub> O	

**Stacking gel**

Rotiphorese™ Gel 30	17%
Tris (pH 6.8)	125 mM
SDS	0.1%
TEMED	0.2%
APS	0.1%
H <sub>2</sub> O	

**Electrophoresis buffer**

Tris	4.9 mM
Glycine	38 mM
SDS	0.1%
H <sub>2</sub> O	

**Tank buffer**

Tris base	48 mM
Glycine	39 mM
Methanol	20%
H <sub>2</sub> O	

**Table 5** Primary antibodies

<b>Antigen</b>	<b>Product no.</b>	<b>Provider</b>	<b>Dilution</b>	<b>In</b>
actin	MAB1501	Millipore	1:1,000	Blotto 1%
Akt	#9272	Cell Signaling Technology	1:1,000	BSA 5%
p-Akt (Ser473)	#9271	Cell Signaling Technology	1:1,000	BSA 5%
p-ATM (Ser794)	ab119799	abcam	1:1,000	BSA 5%
p-ATM (Ser1981)	#5883	Cell Signaling Technology	1:1,000	BSA 5%
p-ATR (Ser428)	#2853	Cell Signaling Technology	1:1,000	BSA 5%
p-BRCA1 (Ser1524)	#9009	Cell Signaling Technology	1:1,000	BSA 5%
p-cdc2 (Tyr15)	#9111	Cell Signaling Technology	1:1,000	BSA 5%
Cdk5	AHZ0492	Invitrogen	1:1,000	Blotto 1%
p-Cdk5 (Tyr15)	EP762RY	Epitomics	1:1,000	BSA 5%
p-Chk1 (Ser345)	#2348	Cell Signaling Technology	1:1,000	BSA 5%

Antigen	Product no.	Provider	Dilution	In
p-Chk2 (Thr68)	#2661	Cell Signaling Technology	1:1,000	BSA 5%
CREB	#9104	Cell Signaling Technology	1:1,000	BSA 5%
p-H2A.X (Ser139)	#2577	Cell Signaling Technology	1:1,000	BSA 5%
p27 <sup>Kip1</sup>	610241	BD Transduction Laboratories	1:1,000	Blotto 1%
p35	sc-820	Santa Cruz Biotechnology	1:500	Blotto 1%
$\beta$ -tubulin	#2146	Cell Signaling Technology	1:1,000	BSA 5%

**Table 6** Secondary antibodies

Antibody	Product no.	Provider	Dilution	in
Goat anti-mouse IgG1: HRP	BZL07046	Biozol	1:1,000	Blotto 1%
Goat anti-rabbit: HRP (H + L)	111-035-144	Dianova	1:1,000	Blotto 1%
Alexa Fluor <sup>®</sup> 680 Goat anti-mouse IgG (H + L)	A - 21057	Molecular Probes	1:10,000	Blotto 1%
IRDye <sup>™</sup> 800CW Goat anti-rabbit IgG (H + L)	926-32211	LI-COR Biosciences	1:10,000	Blotto 1%

## 2.5 Nuclear/cytoplasmic fractionation

Cells were washed once with ice-cold PBS, before additionally PBS is added. Afterwards cells were scraped off carefully, centrifuged (1,500 rpm, 10 min, 4°C) and the cell pellet was resuspended in nuclear extraction buffer A. After incubation on ice for 15 min, Nonidet P-40 (0.625%) was added, followed by vigorous vortexing. Probes were centrifuged (12,000 rpm, 1 min, 4°C) and supernatants as cytoplasmic fraction was removed. The pellet was incubated for 20 min at 4°C in nuclear extraction buffer B. After centrifugation (12,000 rpm, 5 min, 4°C) the supernatant as nuclear fraction was collected. In all fractions protein concentration was determined and adjusted by adding lysis buffer.

Afterwards the samples were either mixed with 5x SDS sample buffer for Western Blot analysis or were further used for immunoprecipitation and kinase activity assay.

**Table 7** Nuclear extraction buffer A and B

<b>Nuclear extraction buffer A</b>		<b>Nuclear extraction buffer B</b>	
HEPES pH 7.9	10 mM	HEPES pH 7.9	20 mM
KCl	10 mM	NaCl	0.4 mM
EDTA	0.1 mM	EDTA	0.1 mM
EGTA	0.1 mM	EGTA	0.1 mM
DTT	1 mM	DTT	1 mM
PMSF	0.5 mM	PMSF	0.5 mM
Complete <sup>®</sup> EDTAfree	1 mM	Complete <sup>®</sup> EDTAfree	1 mM
H <sub>2</sub> O		Glycerol	25%
		H <sub>2</sub> O	

## 2.6 Immunoprecipitation

Cells were harvested with IP lysis buffer (Table 8), scraped off and kept on ice for 30 min. Afterwards samples were centrifuged (14,000 rpm, 10 min, 4°C) and protein concentrations were determined in the supernatants. Cell lysates were incubated with 2 µg antibody (Cdk5; sc-173, Santa Cruz Biotechnology) per 500 µg protein amount over night at 4°C. Thereafter, 25 µL packed Protein G Agarose beads with IP lysis buffer were added to each sample. After 3 h of incubation at 4°C, the beads were spun down and washed three times with lysis buffer.

## 2.7 Kinase activity assay

Beads from Cdk5 immunoprecipitation were resuspended in 50 µL kinase buffer. In addition, 2 µM ATP, 10 µCi <sup>32</sup>P-γ-ATP and 0.05 µg/µL histone H1 (Type III from calf thymus) as a substrate were added to each sample and the enzyme reaction was carried out at 30°C for 20 min. For termination samples were mixed with 5x SDS sample buffer

and boiled for 5 min at 95°C. Aliquots of each sample were loaded onto a 12% SDS PAGE gel and electrophoresis was run. For autoradiography, an X-ray film was placed on the gel for 4 to 48 h at -80°C.

**Table 8** IP lysis buffer and kinase buffer

<b>IP lysis buffer</b>		<b>Kinase buffer</b>	
Tris/HCl pH 7.5	50 mM	HEPES pH	7.0
NaCl	250 mM	MgCl <sub>2</sub>	10 mM
EDTA pH 8.0	1 mM	DTT	1 mM
NaF	10 mM	NaF	1 mM
SIGMAFAST™	1x	Na <sub>3</sub> VO <sub>4</sub>	1 mM
Protease Inhibitor		PMSF	1 mM
H <sub>2</sub> O		β-glycerophosphate	3 mM
		Complete® EDTAfree	4 mM
		H <sub>2</sub> O	

## 2.8 Human HCC microarrays

Tissue microarray (TMA) containing human HCC samples as well as matched surrounding non-tumor tissue was kindly provided by Dr. E. De Toni (Department of Medicine II, University Hospital Großhadern, University of Munich, Germany).<sup>46</sup> The included HCC patients had been treated with liver transplantation or partial hepatectomy at the University Clinic Munich Großhadern between 1985 and 2008.

## 2.9 Immunohistochemistry

### 2.9.1 Cdk5 and Ki-67

5 µm sections of the TMA or tumor tissue from the HUH7 xenografts were used for immunohistochemical staining. The slides were deparaffinized in xylene (15 min) and rehydrated through descending concentrations of ethanol (20 min in 100% and 20 min in

95%). For antigen retrieval sections were boiled in sodium citrate buffer (10 mM sodium citrate, 0.05% Tween 20, pH 6.0) for 20 min. Endogenous peroxidase was blocked by incubation in 7.5% hydrogen peroxide for 10 min. Between the different steps the slides were always washed two times with PBS. Cdk5 antibody (ab40773; abcam) or Ki-67 antibody (ab15580; abcam), diluted 1:100 in PBS, was applied as primary antibody for 1 h at room temperature. For antibody detection Vectastain<sup>®</sup> Universal Elite ABC Kit was taken according to the manual and AEC was used as a chromogen. Slides were counterstained with hematoxylin for 1 min and washed with distilled water. Finally, stained sections were embedded in FluorSave<sup>™</sup> Reagent mounting medium and covered with glass coverslips. Images were obtained with an Olympus BX41 microscope and an Olympus DP25 camera.

### 2.9.2 Terminal deoxynucleotidyl transferase dUTP nick end labeling (TUNEL)

Apoptotic cells in 5  $\mu\text{m}$  sections from tumors derived from HUH7 xenografts were visualized using the ApopTag<sup>®</sup> Plus Fluorescein In Situ Apoptosis Detection Kit according to the manual. Cell nuclei were counterstained with 5  $\mu\text{g}/\text{mL}$  Hoechst 33342 in PBS containing 1% BSA for 60 min. Stained sections were mounted with FluorSave<sup>™</sup> Reagent mounting medium. Images were obtained with a Zeiss LSM 510 Meta confocal laser scanning microscope.

## 2.10 Immunostaining

HCC cells were seeded in 8-well ibiTreat  $\mu$ -slides. Afterwards, cells were washed once with ice-cold PBS+Ca<sup>2+</sup>/Mg<sup>2+</sup> and fixed in 4% formaldehyde for 15 min, following one washing step with PBS. For permeabilization 0.2% Triton X-100 in PBS was applied for 2 min. After washing with PBS, unspecific binding was blocked by incubation with 0.2% BSA in PBS for 20 min. Cells were incubated with the primary antibody against Cdk5 (AHZ0492; Invitrogen), p27<sup>Kip1</sup> (610241; BD Transduction Laboratories), Ki-67 (ab15580, abcam) and p-H2A.X (#2577; Cell Signaling Technology), diluted 1:100 in PBS containing 0.2% BSA, for 1 h. Afterwards, cells were washed with PBS and incubated with Alexa Fluor<sup>®</sup> 488 or 546-conjugated secondary antibody (Invitrogen), diluted 1:400, together with 5  $\mu\text{g}/\text{mL}$  Hoechst 33342 in PBS containing 0.2% BSA for 30 min. After washing again with

PBS, stained cells were covered with FluorSave™ Reagent mounting medium and glass coverslips. Images were obtained with a Zeiss LSM 510 Meta confocal laser scanning microscope.

## 2.11 Proliferation assays

### 2.11.1 Crystal violet staining

HCC cells were seeded into 96-well plates. After 24 h incubation, cells in a reference plate were stained with crystal violet, serving as initial cell number. The cells in the remaining plates were either left untreated or stimulated with increasing concentrations of roscovitine. Upon an incubation period of 72 h, the medium was removed and cells were stained with 100  $\mu$ L crystal violet solution for 10 min at room temperature. After washing with distilled water, the bound dye was solubilized by adding 100  $\mu$ L of dissolving buffer. The absorbance was measured at 550 nm in a plate-reading photometer.

**Table 9** Crystal violet solution and dissolving buffer

Crystal violet solution		Dissolving buffer	
Crystal violet	0.5%	Trisodium citrate	50 mM
Methanol	20%	Ethanol	50%
H <sub>2</sub> O			

### 2.11.2 Impedance measurement

Proliferation of HCC cells with stable Cdk5 knockdown was determined using the xCELLigence System from Roche Diagnostics. HUH7 cells were seeded at a density of 2,000 cells per 100  $\mu$ L in equilibrated E-plates. After synchronizing the cells by treatment with 10  $\mu$ M aphidicolin for 24 h, cells were either left untreated or treated with different substances as indicated for 72 h. The cell index, which is proportional to the cell number, was measured every hour and normalized to the value at the time of aphidicolin release. In the end the doubling time was evaluated by the xCELLigence software.

## 2.12 Colony formation assay

The colony formation assay is an *in vitro* long term cell survival assay to determine the effectiveness of cytotoxic agents based on the ability of a single cell to form a colony. HCC cells were seeded into 6-well plates and treated as indicated for 24 h. Subsequently, cells were trypsinized and reseeded in fresh medium with 10,000 cells per well in 6-well plates. Upon an incubation period of 7 d, cells were stained with crystal violet solution (Table 9) for 10 min at room temperature. After washing with distilled water, the bound dye was solubilized by adding 1 ml dissolving buffer (Table 9). The absorbance was measured at 550 nm in a plate-reading photometer.

## 2.13 Motility assays

### 2.13.1 Boyden Chamber assay

Transwell<sup>®</sup> permeable supports (8  $\mu$ m pore polycarbonate inserts) were used according to the manufacturer's instructions. The transwell inserts were coated with collagen G to measure the migration and with Matrigel<sup>®</sup> to measure the invasion of tumor cells. Inserts were added to 24-wells containing 700  $\mu$ L DMEM (negative control) or DMEM containing 10% FCS. 100,000 cells in DMEM or DMEM containing indicated agents were added to the inside compartments and allowed to migrate for 16 h. Afterwards cells on both sides of the insert were stained by crystal violet. Cells on the upper side were removed by using cotton swabs and cells attached to the bottom were photographed using a Zeiss Axiovert 25 microscope and a Canon 450D camera. Eight pictures for each sample were taken and the number of cells was counted.

### 2.13.2 Wound healing assay

In the wound healing assay, also called scratch assay, a confluent cell monolayer is wounded and the ability of the cells to migrate and close the artificial scratch is determined. HCC cells were seeded in 24-well plates. After reaching confluence, cells were scratched using a pipette tip of a micropipette. The wounded monolayers were washed twice with PBS to remove floating cellular debris before adding fresh medium or medium containing roscovitine. After about 24 h of migration, cells were washed with PBS

and fixed with 4% formaldehyde. As a negative control cells were fixed directly after scratching. Images of the fixed cells were taken using an imaging system (TILL Photonics GmbH, Gräfelfing, Germany) and a CCD-camera connected to an Axiovert 200 microscope. Images were analyzed using specific software (S.CO LifeScience, Garching, Germany). Migration was quantified as the ratio of the number of pixels in the area covered with cells (green) and the number of pixels in the cell-free area (gray) (Figure 4).

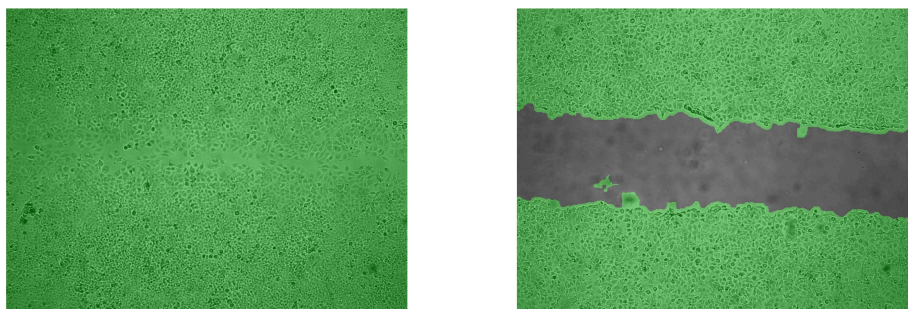


**Figure 4** **Scratch assay.** Images represent fixed HUH7 cells after 27 h of migration treated with growth medium (left panel) or fixed HUH7 cells directly after scratching (right panel).

## 2.14 Cell cycle and apoptosis analysis

Cell cycle analysis and quantification of apoptosis rate was performed according to Nicoletti *et al.*<sup>47</sup>

If specified, cells were synchronized by treatment with 10  $\mu$ M aphidicolin for about 24 h before measuring the cell cycle. Cells were treated as indicated for 24 h to 72 h and afterwards trypsinized, washed with PBS, and centrifugated at 600 g and 4°C for 10 min. For permeabilization and staining, cells were incubated in fluorochrome solution (FS) buffer containing propidium iodide (PI) to detect the DNA content of the cells. After incubation overnight at 4°C, cells were analyzed by flow cytometry on a FACSCalibur.

**Table 10** FS buffer containing PI

### FS buffer

Propidium iodide	75 $\mu$ M
Trisodium citrate	0.1%
Triton-X 100	0.1%
PBS	

The respective fluorescence intensity gives information about the DNA content of a cell, and thus, about rate of apoptosis and cell cycle phases. Apoptotic cells are characterized by DNA fragmentation, indicated by a sub G1 peak. The cell cycle consists of mitosis (M phase) and interphase. The interphase is subdivided into G1/G0-phase, S-phase, and G2-phase, characterized by their DNA contents. The respective fluorescence intensities of cell populations result in characteristic histogram plots (Figure 5).

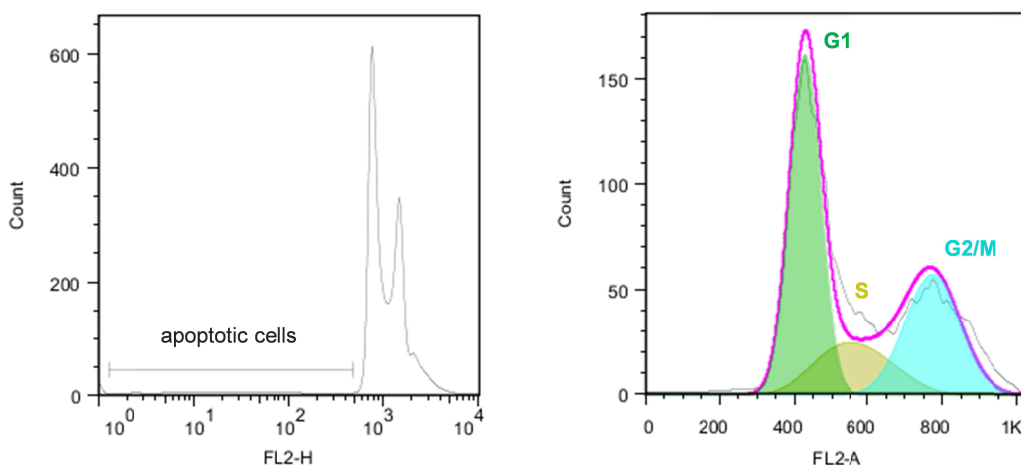


**Figure 5** Analysis of apoptotic cells and cell cycle.

Distribution of cells in distinct cell cycle phases and percentage of apoptotic cells were determined using FlowJo 7.6 analysis software (Tree Star Inc., Ashland, USA).

## 2.15 *In vivo* assays

All experiments were performed according to German legislation for the protection of animals and approved by the local government authorities. All *in vivo* experiments were performed by J. Liebl and B. Hager.

### 2.15.1 Animals

Female SCID mice (8–10 weeks) were housed in individually ventilated cages under specific pathogen free conditions with a 12 h day/night cycle and with free access to food and water.

### 2.15.2 Tumor cell implantation

Normal HUH7 cells or HUH7 cells with Cdk5 knockdown were harvested at about 70% confluency and  $3.3 \times 10^6$  cells in 100  $\mu$ l PBS were injected subcutaneously into the flank of SCID mice. The number of animals per group is indicated in the corresponding figure legend.

Animals were checked regularly for tumor progression. Tumor volume was determined using a digital measuring slide (Digi-Met, Preisser, Gammertingen, Germany). Each measurement consisted of three parameters, length (a), width (b) and height (c) and tumor volume was calculated by the formula  $a \cdot b \cdot c \cdot \pi/6$  (with a, b and c indicating the three parameters and  $\pi/6$  as correction factor for tumor shape).

### 2.15.3 Intraperitoneal application of roscovitine and irinotecan

Roscovitine and irinotecan were injected intraperitoneally (100  $\mu$ L; solvent: PBS/DMSO/Solutol 17:1:2). For roscovitine treatment alone, application was carried out every day with 150 mg/kg (body weight)/d for seven days, beginning seven days after implantation. In the combinatorial treatment, the injections began ten days after implantation with 150 mg/kg/d roscovitine injected 3-times and 10 mg/kg/d irinotecan 2-times per week for 4 weeks.

### 2.15.4 Isolation of tumors

For investigation of tumor size mice were sacrificed by neck fracture. Tumors were removed and weight and volume was determined. Afterwards tumors were fixed with 4% paraformaldehyde in PBS for one day and with 1% paraformaldehyde for additional three days prior to embedding in paraffin.

## 2.16 Statistical analysis

All experiments were performed at least three times unless otherwise indicated in the figure legend. Data are expressed as mean  $\pm$  SEM. Statistical analysis was performed with SigmaPlot<sup>®</sup> software version 10.0 (Systat Software Inc., Chicago, USA). Statistical tests are indicated in the figure legend. Statistical significance was considered if  $p < 0.05$ .

## **RESULTS**

## 3 RESULTS

### 3.1 Cdk5 expression is increased in human HCC

Analysis of Cdk5 in a human HCC tissue microarray<sup>46</sup> (Figure 6A) was performed in cooperation with Prof. Dr. med. Thomas Kirchner and Prof. Dr. med. Doris Mayr from the Institute of pathology and Dr. med. Enrico de Toni from the Department of Internal Medicine II of the University of Munich. The evaluation of the microarray revealed an increased expression of Cdk5 in human HCC (41.3% with high Cdk5 expression; n=179) in comparison to corresponding normal liver tissue (26.4% with high Cdk5 expression; n=174). This was confirmed by immunoblots of HCC and corresponding normal liver patient samples, where expression of Cdk5 and its activator p35, was increased in HCC (Figure 6B). In line, the HCC cell lines HepG2 and HUH7, which were used for further studies, showed expression of Cdk5 and p35 (Figure 6C) and Cdk5 activity (Figure 6D).

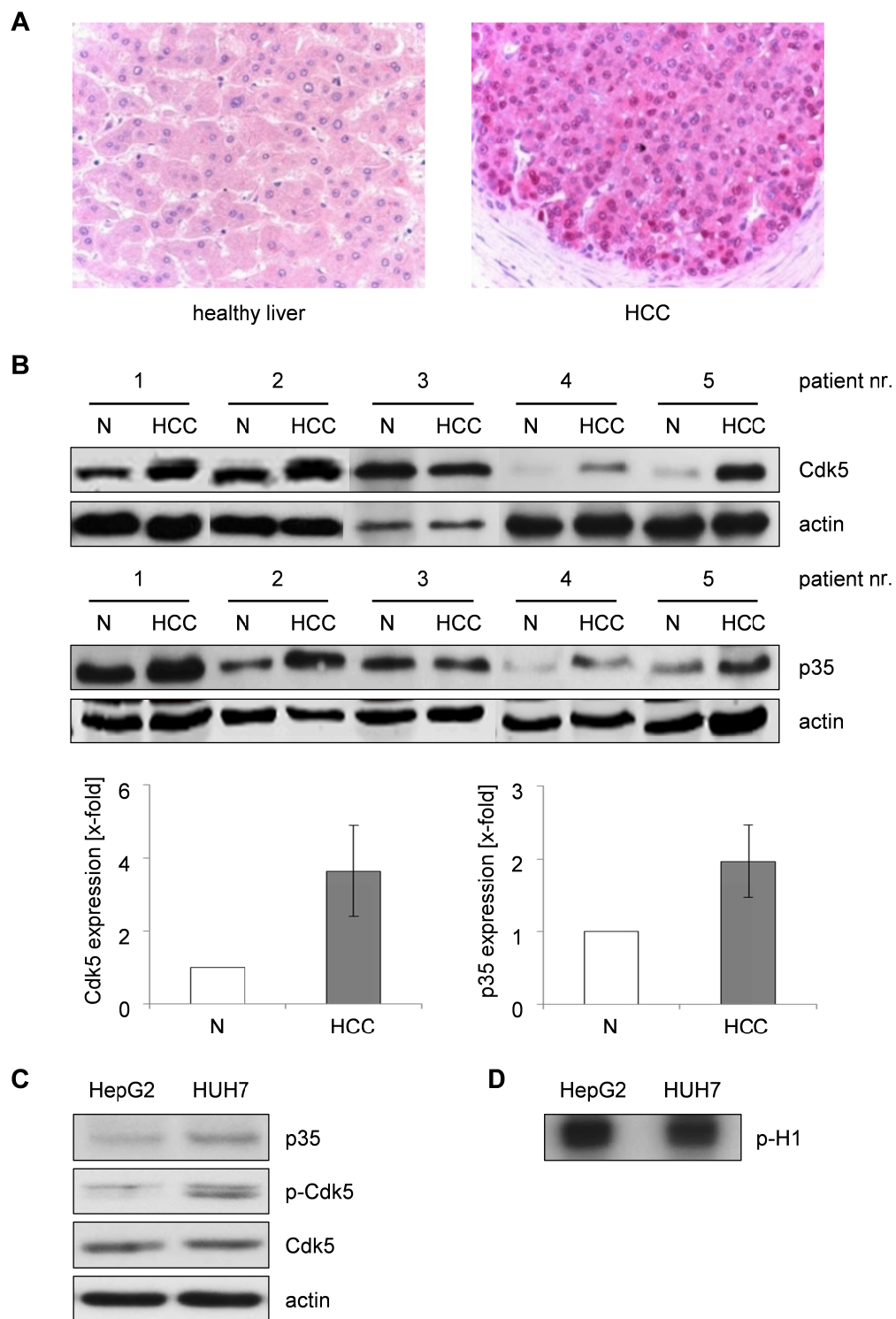
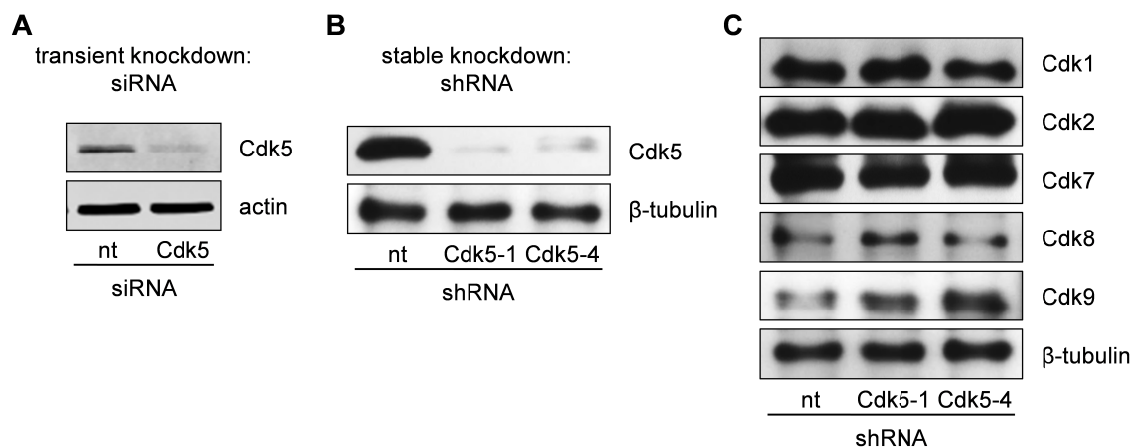


**Figure 6** **Elevated expression of Cdk5 and p35 in human HCC.** (A) Immunostaining of HCC and corresponding healthy liver tissue of a human tissue microarray with staining for Cdk5 (red) and nuclei (blue) is shown. (B) Patient samples of HCC and normal (N) liver tissue were analyzed by Western blot for Cdk5 and p35 expression. Representative immunoblots and combined quantitative evaluation are shown. (C) Immunoblots show the expression of Cdk5 and p35, and phosphorylation of Cdk5 at Tyr15 in different HCC cell lines. (D) Cdk5 activity was determined by radioactive kinase assay. Level of phosphorylated (P-32) histone 1 (p-H1) correlates with Cdk5 activity.

## 3.2 Abrogation of Cdk5 inhibits HCC progression *in vitro* and *in vivo*

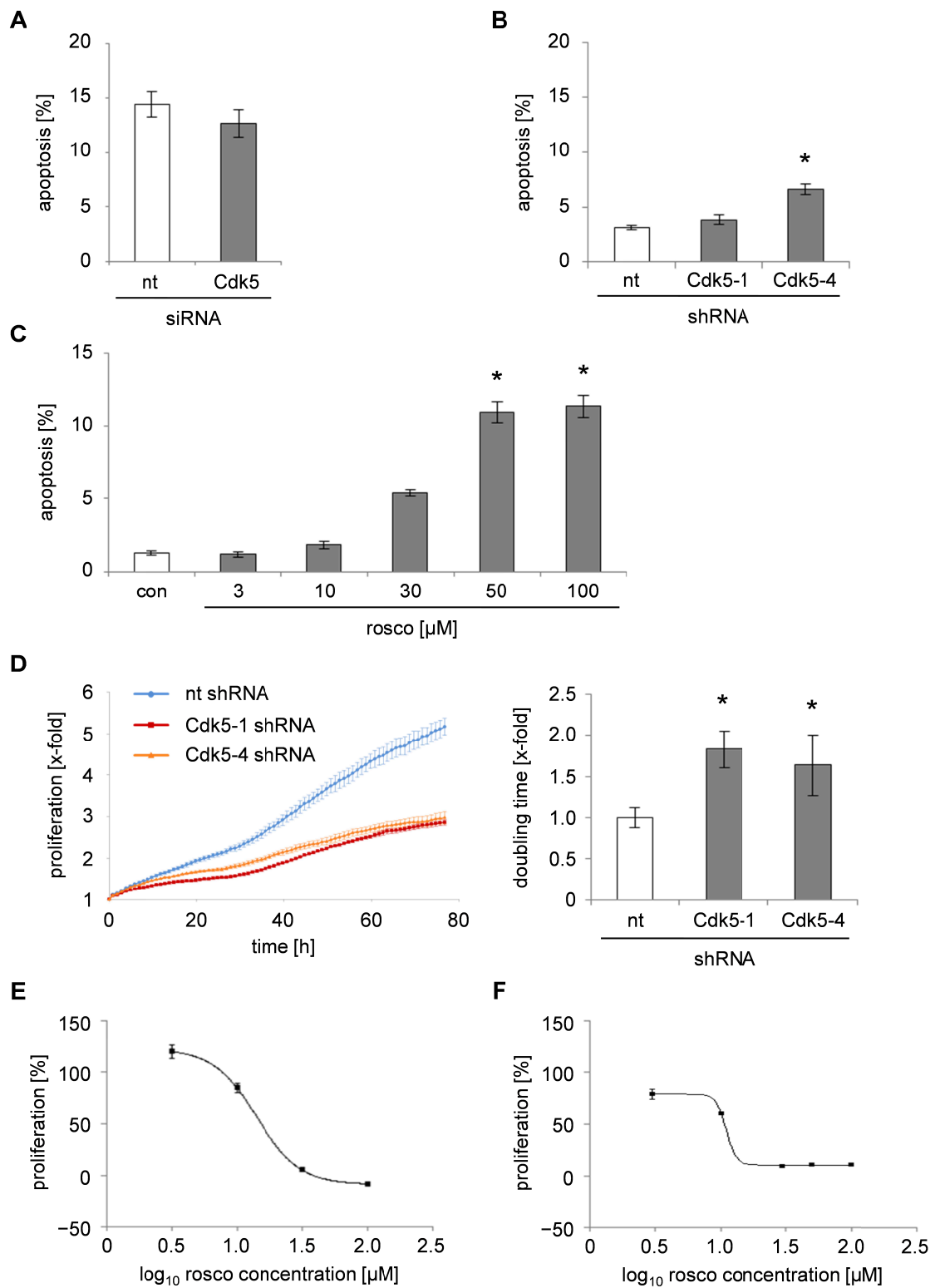
### 3.2.1 Blockage of Cdk5 function inhibits HCC cell growth and motility *in vitro*

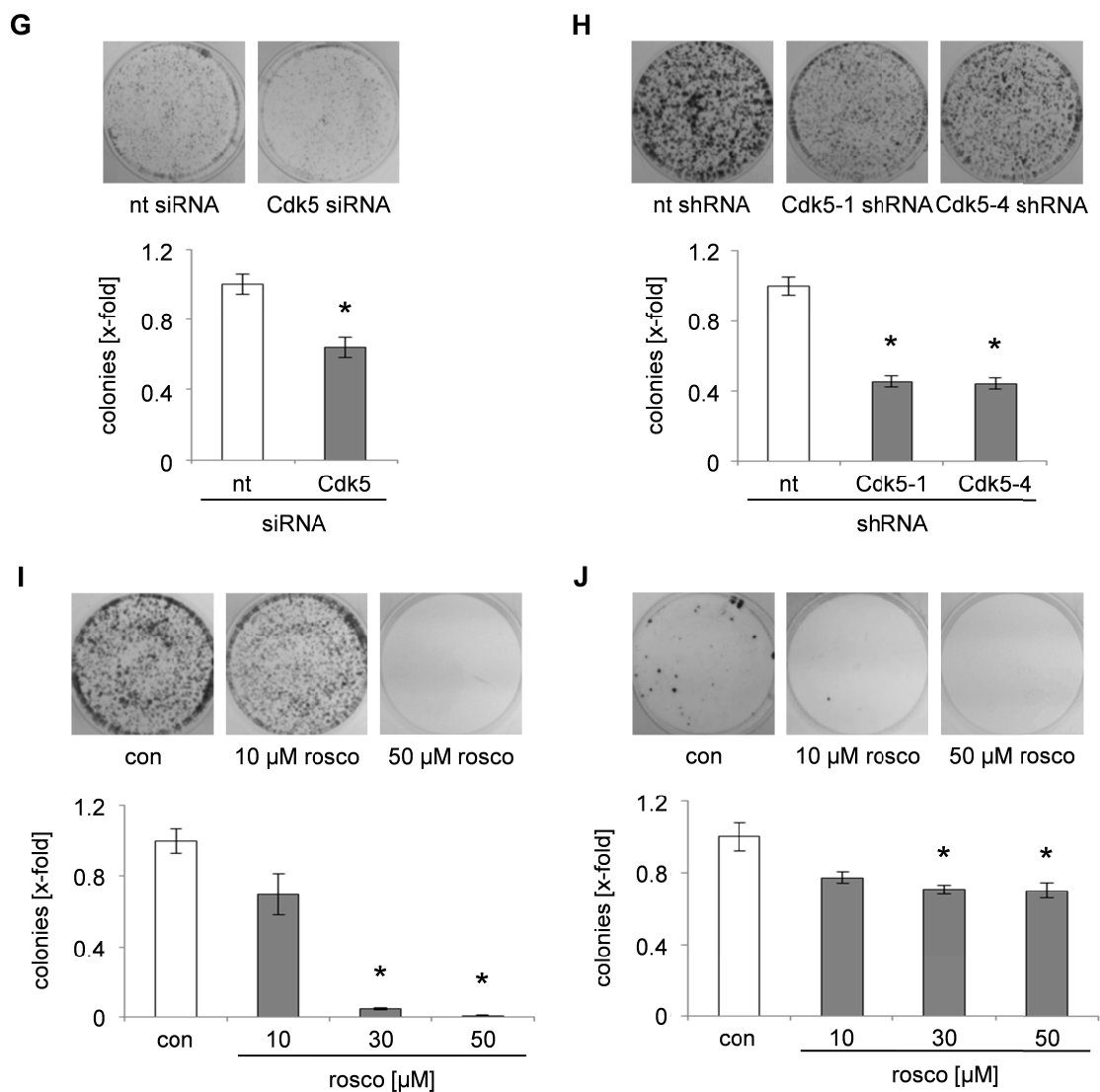
To characterize the function of Cdk5 in HCC, we used pharmacologic inhibition of Cdk5 by roscovitine, as well as genetic downregulation, *i.e.* transient silencing (siRNA) and stable knockdown (shRNA) of Cdk5 (Figure 7A, B) in several functional assays. Stable Cdk5 knockdown cell lines were generated and two independent clones (“Cdk5-1” and “Cdk5-4”) with optimal downregulation of Cdk5 and no influence on other Cdks were picked (Figure 7B, C).



**Figure 7 Cdk5 knockdown by siRNA and shRNA.** (A) Immunoblots from nt and Cdk5 siRNA treated HUH7 cells probed with antibodies for Cdk5 and actin are shown. (B, C) Immunoblots from nt and Cdk5 shRNA treated HUH7 cells probed with antibodies for (B) Cdk5, (C) Cdk1, Cdk2, Cdk7, Cdk8, Cdk9 and  $\beta$ -tubulin are shown.

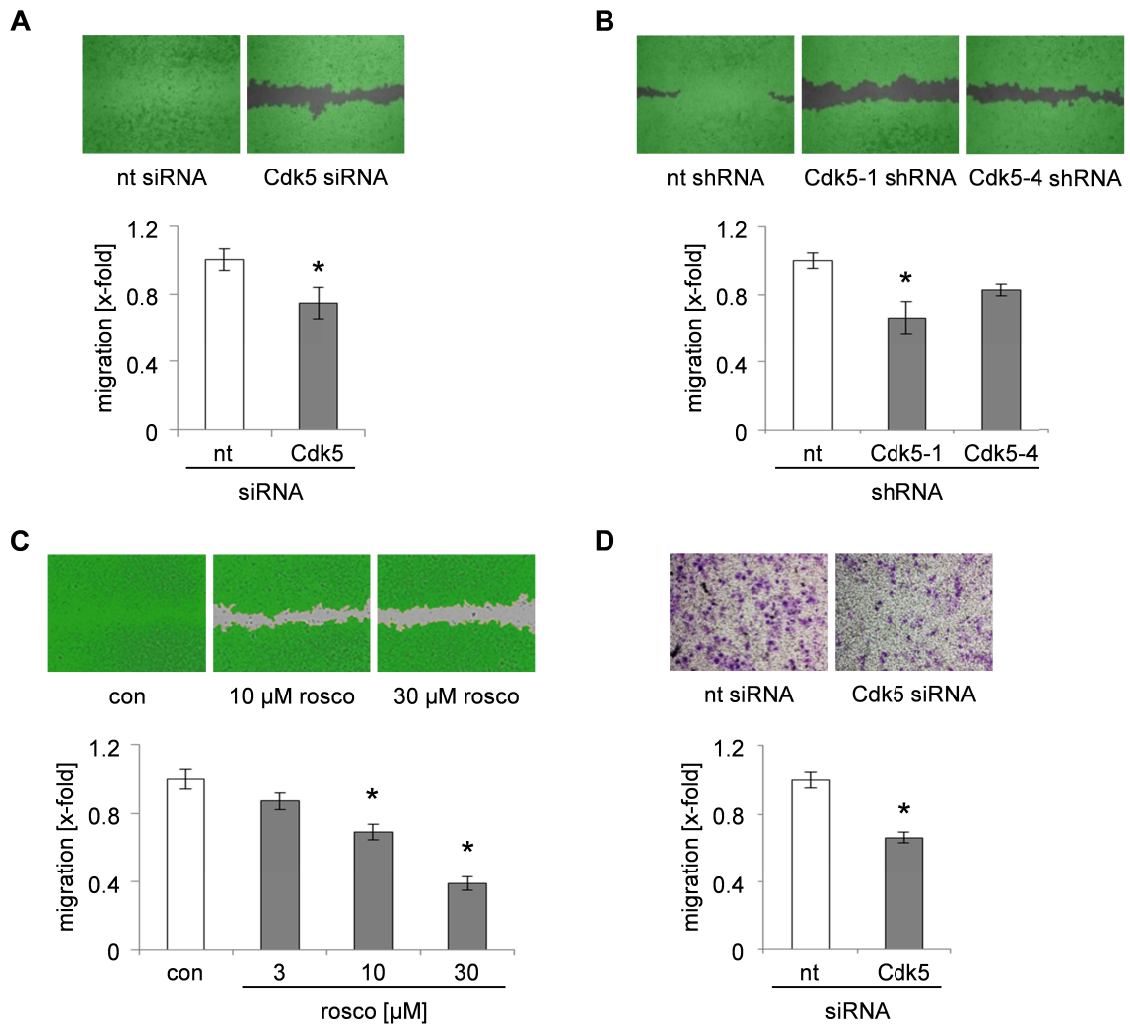
Blockade of Cdk5 function had only moderate effect on apoptosis induction in HUH7 cells after 72 h (Figure 8A-C). In contrast, Cdk5 knockdown as well as pharmaceutical inhibition by roscovitine decreased proliferation of HCC cells (Figure 8D-F). Of note, clonogenic survival was also significantly reduced by Cdk5 siRNA, shRNA and roscovitine (Figure 8G-J).





**Figure 8 Genetic downregulation and pharmacological inhibition of Cdk5 decreases HCC cell proliferation and clonogenic survival.** (A, B) Apoptosis rate of (A) nt and Cdk5 siRNA HUH7 cells and (B) nt and Cdk5 shRNA HUH7 cells after 72 h is shown. (One Way ANOVA on Ranks, Dunn's  $*p < 0.05$ ,  $n = 3$ ). (C) Apoptosis rate of HUH7 cells treated with roscovitine at indicated concentrations for 72 h is shown. (One Way ANOVA on Ranks, Dunn's  $*p < 0.05$ ,  $n = 3$ ). (D) Proliferation of nt and Cdk5 shRNA HUH7 cells after synchronization by aphidicolin and corresponding doubling time is shown. (One Way ANOVA, Holm-Sidak  $*p < 0.05$ ,  $n = 3$ ). (E) Proliferation of HUH7 cells treated with roscovitine at indicated concentrations for 72 h is shown.  $EC_{50} = 14.2 \mu\text{M}$ . (F) Proliferation of HepG2 cells treated with Roscovitine at indicated concentrations is shown.  $EC_{50} = 10.9 \mu\text{M}$ . (G, H) Clonogenic survival of (G) nt and Cdk5 siRNA as well as of (H) nt and Cdk5 shRNA HUH7 cells is shown. (G) (t-test  $*p < 0.001$ ,  $n = 4$ ). (H) (One Way ANOVA, Holm-Sidak  $*p < 0.05$ ,  $n = 3$ ). (I) Clonogenic growth of HUH7 cells that were either left untreated (con) or treated with roscovitine for 24 h and freshly seeded for 7 days is displayed. (One Way ANOVA on Ranks, Dunn's  $*p < 0.05$ ,  $n = 3$ ). (J) Clonogenic growth of HepG2 cells treated with roscovitine is shown. (One Way ANOVA on Ranks, Dunn's  $*p < 0.05$ ,  $n = 3$ ).

Influence on cell motility was determined by wound healing and transwell migration assays. Both assays revealed that Cdk5 is essential for HCC cells migration on a 2D surface (Figure 9A-C). and also through small pores (Figure 9D, E). By coating the membrane of Boyden Chambers with Matrigel<sup>®</sup>, it is possible to simulate the invasion of cancer cells through extracellular matrix. Importantly, the invasion was also significantly reduced by Cdk5 knockdown (Figure 9F).



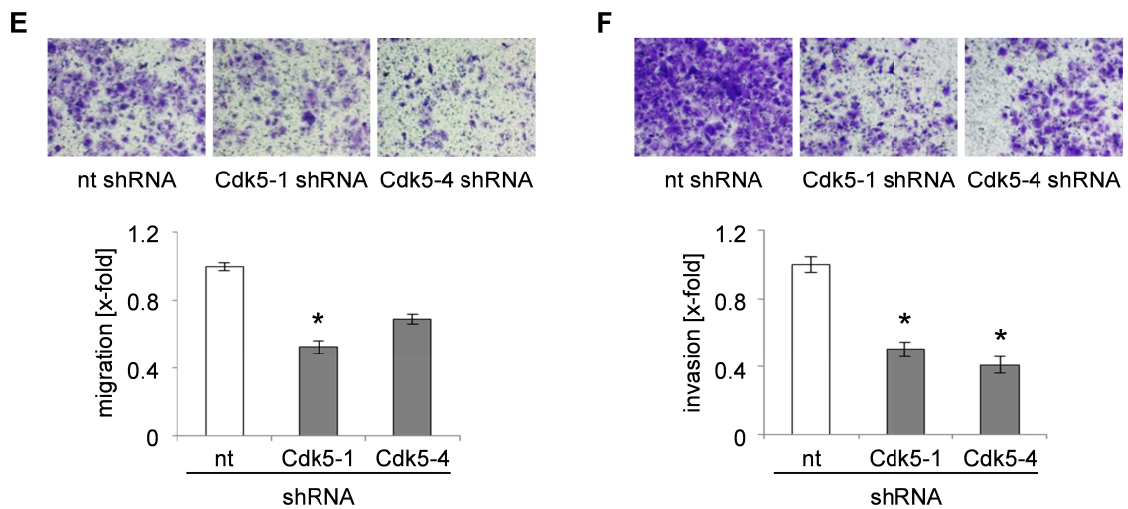


**Figure 9** Transient or stable knockdown of Cdk5 as well as treatment with roscovitine inhibit HCC cell motility and invasion. (A) Wound healing assays of HUH7 cells transfected with nt or Cdk5 siRNA is shown. Migration is shown as ratio of pixels covered by cells and pixels of the cell free wound. (t-test  $*p < 0.05$ ,  $n = 5$ ). (B) Wound healing assay of nt shRNA and Cdk5 shRNA HUH7 cells is displayed. (One Way ANOVA on Ranks, Dunn's  $*p < 0.05$ ,  $n = 3$ ). (C) Wound healing assays of HUH7 cells that have been either left untreated (con) or treated with roscovitine for 27 h is shown (right panel). (One Way ANOVA, Holm-Sidak  $*p < 0.05$ ,  $n = 3$ ). (D, E) Transwell migration of (D) nt and Cdk5 siRNA treated HUH7 cells as well as (E) nt shRNA and Cdk5 shRNA HUH7 cells was determined by Boyden Chamber assays. The graph displays the number of migrated cells related to control. (t-test  $*p < 0.05$ ,  $n = 3$ ). (One Way ANOVA on Ranks, Dunn's  $*p < 0.05$ ,  $n = 3$ ). (F) Invasion of nt and Cdk5 shRNA HUH7 cells is shown. (One Way ANOVA, Holm-Sidak  $*p < 0.05$ ,  $n = 3$ ).

### 3.2.2 Inhibition of Cdk5 reduces HCC tumor growth in a xenograft mouse model

To evaluate the role of Cdk5 in HCC *in vivo*, we applied a HCC xenograft with genetic downregulation and pharmacologic inhibition of Cdk5. The tumors established from stable Cdk5 knockdown HUH7 cells were significantly smaller compared with the control tumors (Figure 10A-C). Roscovitine treatment also led to a decreased tumor growth *in vivo* (Figure 10D-F).

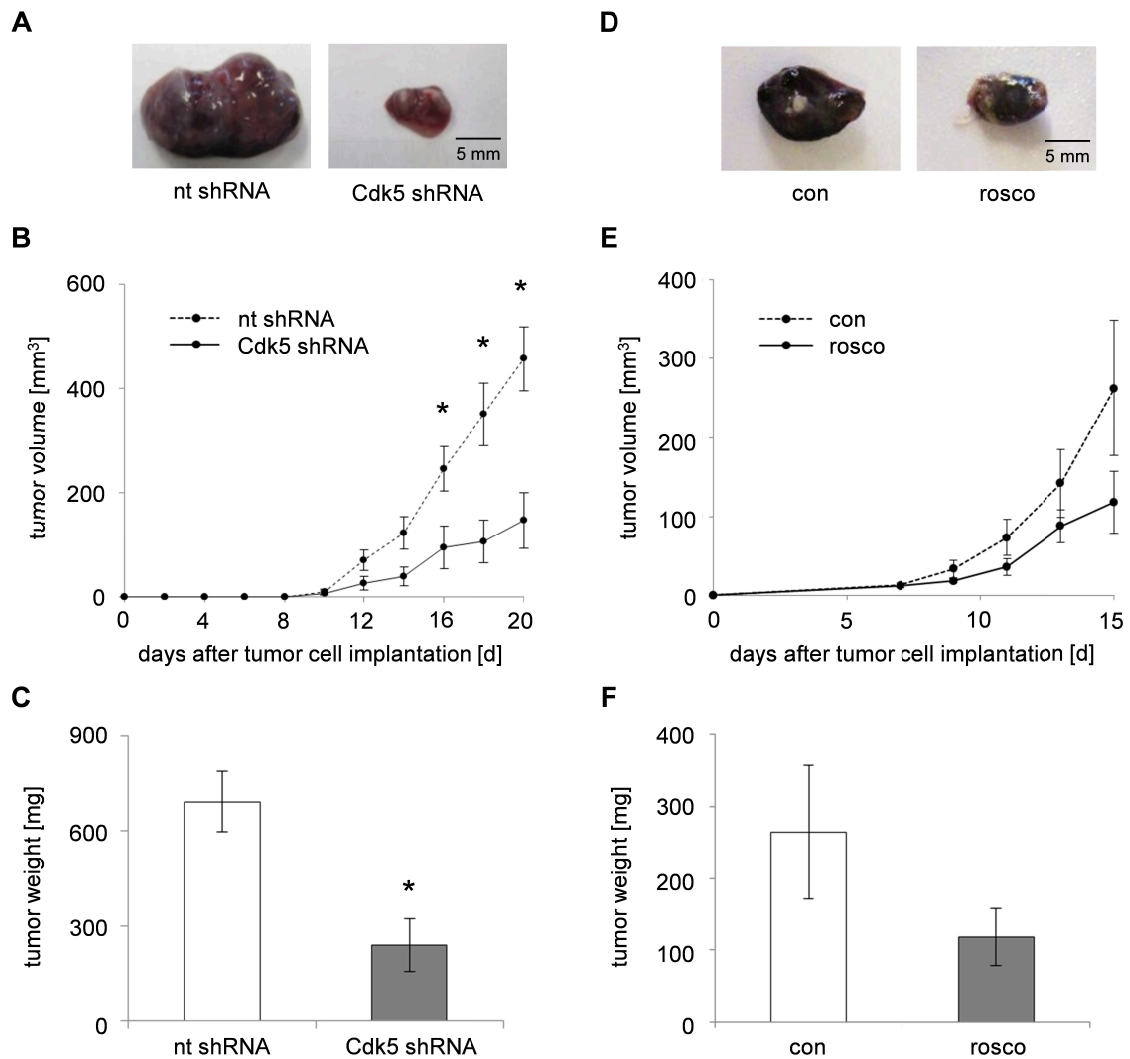


**Figure 10** Inhibition or distinct knockdown of Cdk5 reduces HCC growth *in vivo*. (A, B) Tumors of nt shRNA and Cdk5 shRNA HUH7 cells grown in SCID mice are shown. Tumor volume was monitored over time. (t-test \*p<0.05; n=11). (C) Tumor weight after dissection is shown. (t-test \*p<0.05). (D, E) Displayed tumors of HUH7 cells were derived from mice, which were either left untreated (con) or treated with roscovitine. Tumor volume over time and (F) tumor weight after dissection is shown. (n=8).

This reduction in tumor size was not due to an increased apoptosis of HCC cells (Figure 11A, B). However, staining of proliferating cells in both experiments, using the proliferation marker Ki-67, revealed a decreased percentage of proliferating HCC cells after inhibition or knockdown of Cdk5 (Figure 11C, D). This was consistent with the phenotype observed *in vitro*. Loss of Cdk5 function in HCC cells was associated with significantly reduced tumorigenicity *in vivo*.

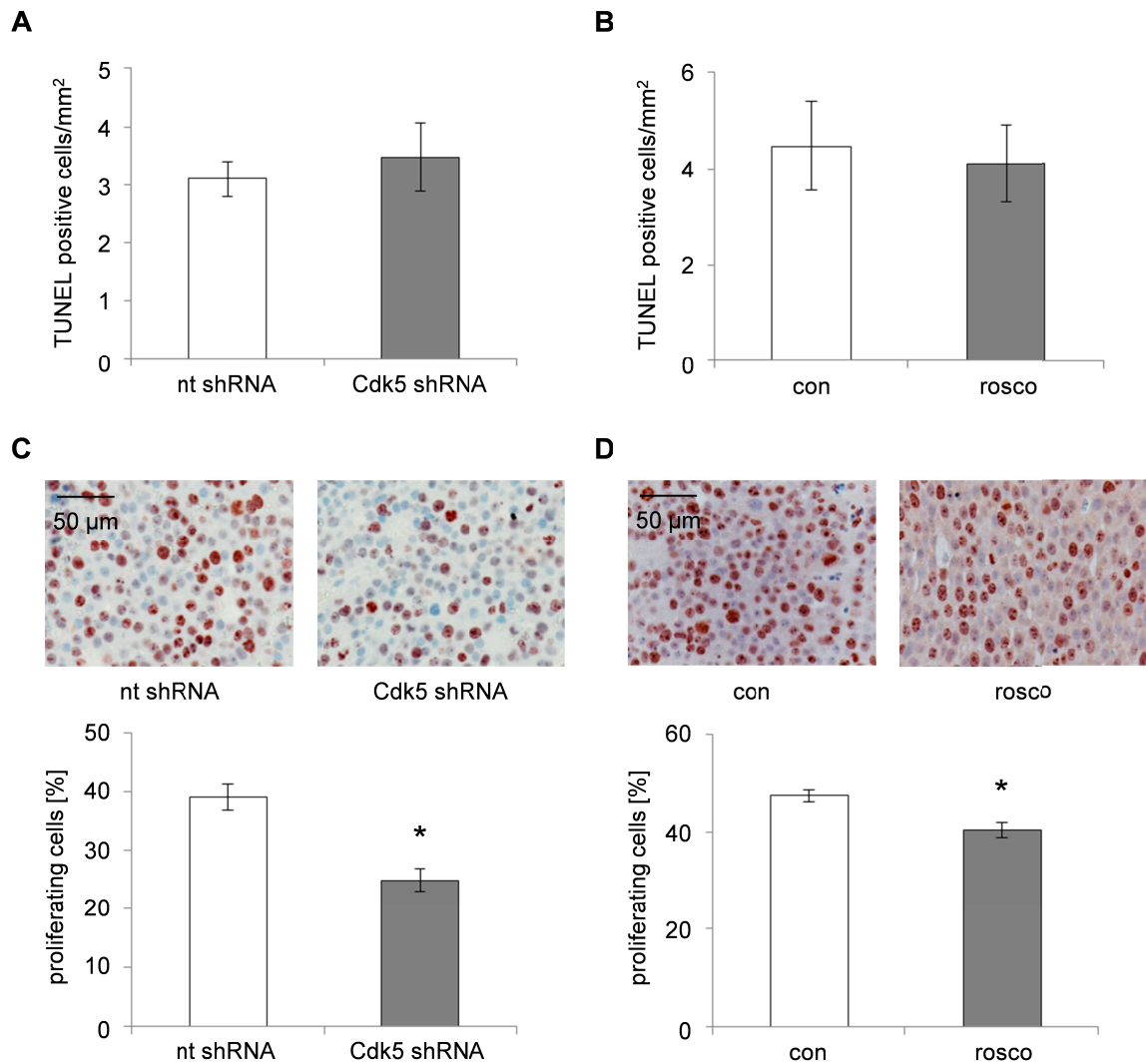
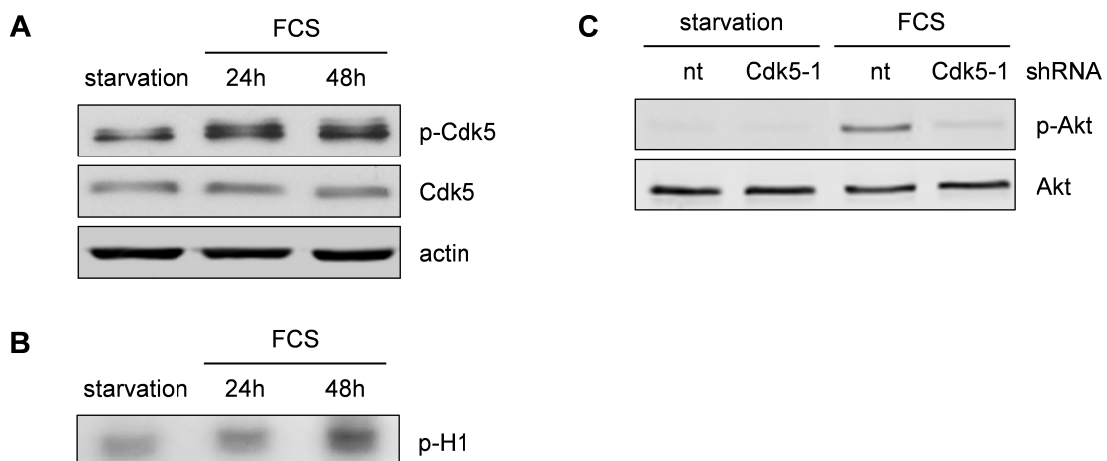


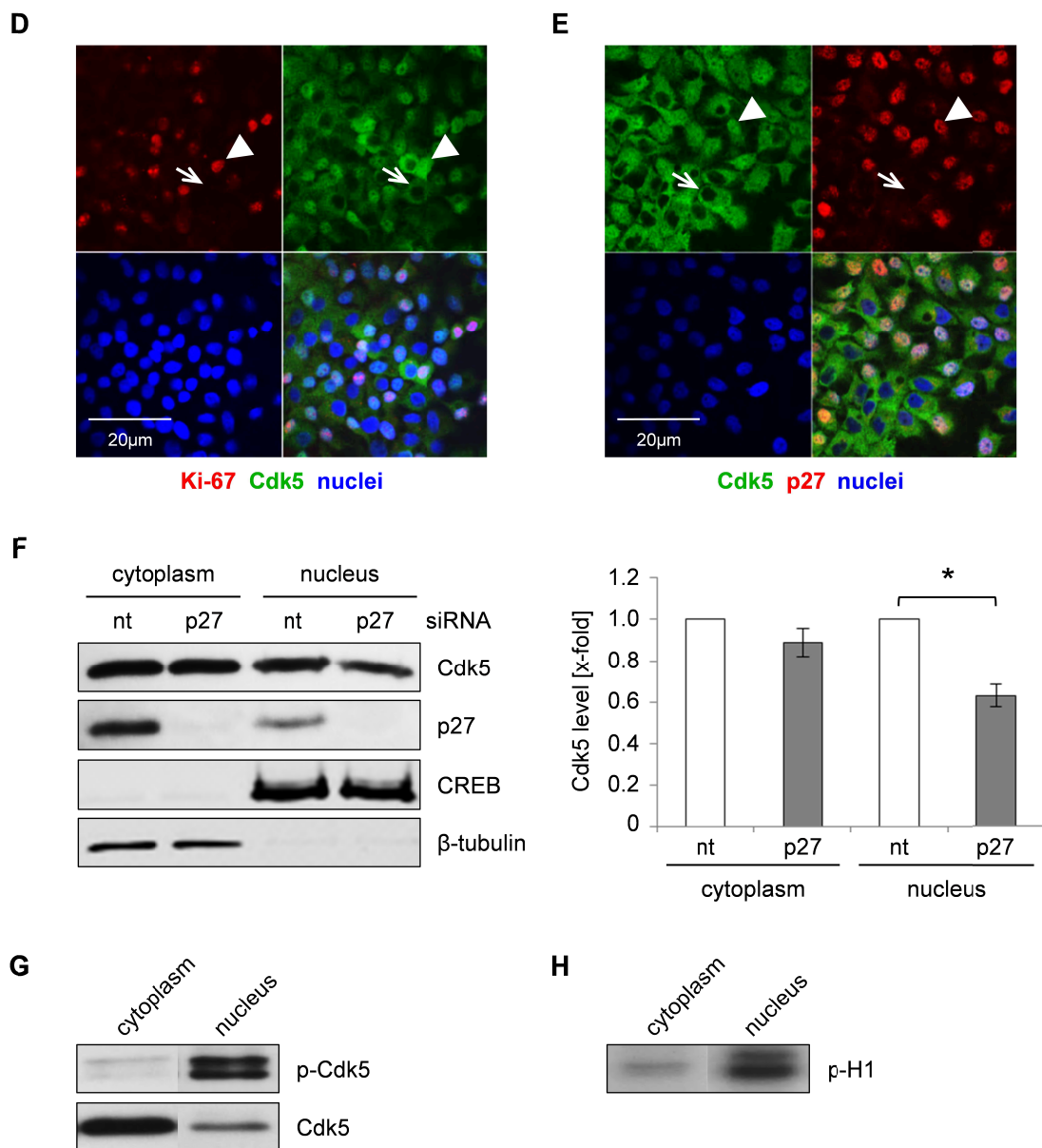
**Figure 11 HCC cell proliferation is decreased by inhibition or distinct knockdown of Cdk5 *in vivo*.** (A, B) Apoptotic cells in indicated tumors were determined by TUNEL labeling. Quantification of TUNEL positive cells is shown. (C, D) Immunostaining for Ki-67 (red) and nuclei (blue) in indicated tumors was quantified to determine the percentage of proliferating cells. (C) (t-test \* $p < 0.05$ ;  $n = 11$ ). (D) (t-test \* $p < 0.05$ ;  $n = 7$ ).

### 3.3 Function of Cdk5 in the nucleus of HCC cells

#### 3.3.1 Cdk5 is localized in the nucleus of proliferating HCC cells

So far our data point to a distinct effect of Cdk5 on HCC proliferation. Thus, we aimed to elucidate the underlying mechanism behind Cdk5's influence on HCC cell proliferation. Serum (FCS) driven stimulation of cell growth led to an enhanced phosphorylation and activation of Cdk5 (Figure 12A, B). Cdk5 knockdown cells showed a reduced FCS-induced phosphorylation of Akt, which is one of the most prominent protein involved in cell proliferation (Figure 12C). Interestingly, proliferating HCC cells, visualized by staining for the established proliferation marker Ki-67, displayed Cdk5 in the cytoplasm as well as in the nucleus. However, HCC cells which did not reproduce (Ki-67 negative) had no Cdk5 in their nuclei (Figure 12D). Further, nuclear location of Cdk5 was dependent on nuclear p27 colocalization (Figure 12E), as downregulation of p27 led to significant less Cdk5 in the nucleus (Figure 12F). Thus Cdk5 localization in the nucleus seems to be a regulated process in HCC similar to what has been observed in neurons.<sup>48</sup> Of note, nuclear Cdk5 is highly active as indicated by a higher ratio of phosphorylated Cdk5 at Tyr15 to total Cdk5 compared to Cdk5 in the cytoplasm (Figure 12G) as well as a higher Cdk5 activity in the nucleus (Figure 12H). These findings together indicate an important function of Cdk5 in the nucleus of proliferating HCC cells.

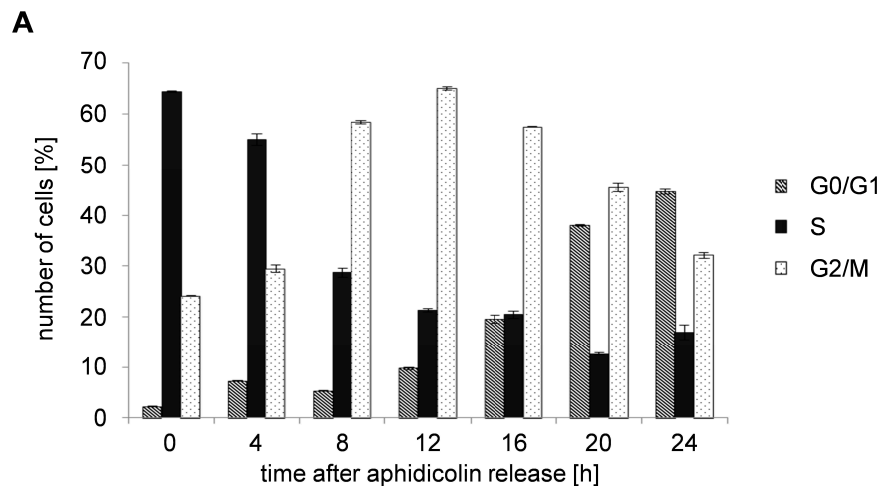


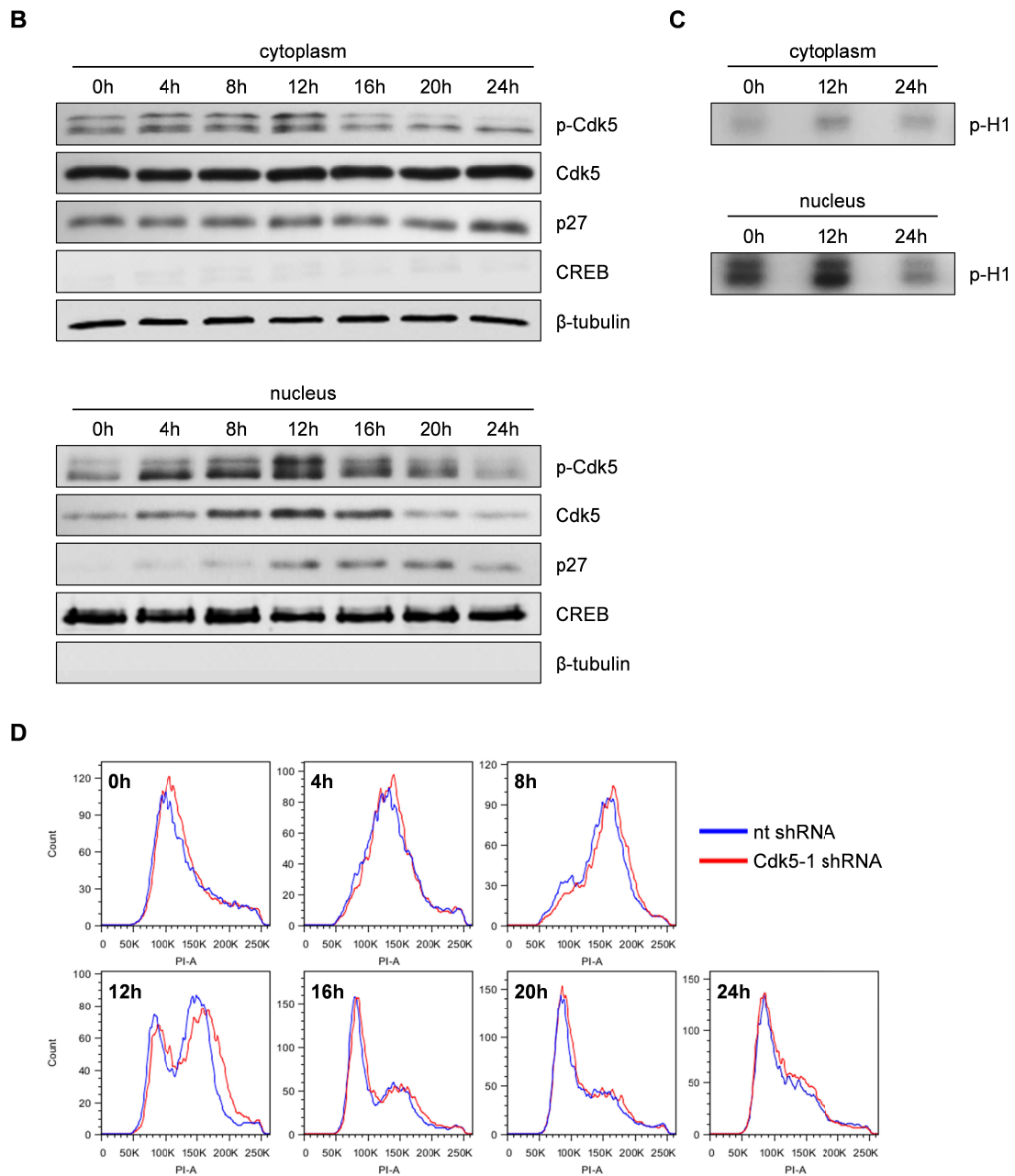


**Figure 12 Cdk5 is activated and localized in the nucleus of proliferating cells.** (A) Cdk5 expression and phosphorylation (Tyr15) was investigated after stimulation with 10% FCS by Western blot analysis. (B) Cdk5 activity was determined by radioactive kinase assay after stimulation with 10% FCS for indicated times. (C) Immunoblots from nt and Cdk5 shRNA HUH7 cells treated with FCS as indicated show p-Akt (Ser473) and total Akt protein levels. (D) Immunostaining for Cdk5 (green), Ki-67 (red) and Hoechst33342 (blue) is shown. Arrowheads indicate nuclear Cdk5 localization in Ki-67 positive cells. Arrows indicate absence of nuclear Cdk5 in Ki-67 negative cells. (E) Immunostaining for Cdk5 (green), p27 (red) and Hoechst33342 (blue) is shown. Arrowheads indicate localization of Cdk5 and p27 in the nucleus. Arrows indicate absence of Cdk5 and p27 in the nucleus. (F) HUH7 cells were transfected with p27 siRNA and afterwards nuclear and cytoplasmic fractions were analyzed for p27 and Cdk5 protein levels by Western blot. CREB and  $\beta$ -tubulin are shown as fractionation controls. Representative blot and combined quantitative evaluation is shown. (One Way ANOVA, Holm-Sidak  $*p < 0.05$ ,  $n = 3$ ). (G) Western blot and (H) Cdk5 activity assay was performed from nuclear and cytoplasmic fractions of HUH7 cells.

### 3.3.2 Cdk5 is activated in the nucleus of cells in the G2/M cell cycle phase

As Cdk5 seems to be important in the nucleus of proliferating cells, we further investigated whether the distribution of Cdk5 is affected by cell cycle progression. Therefore HUH7 cells were synchronized using aphidicolin and after release localization, expression and phosphorylation of Cdk5 and p27 were analyzed at different time points. At the same time, the cell cycle progression of these cells was monitored (Figure 13A). In the cytoplasm almost no difference in the protein levels was detected during the cell cycle. Of note, the levels of nuclear Cdk5 together with its nuclear binding protein p27 show a wave-like pattern (Figure 13B). They increase up to 12 h after aphidicolin release, at which time point most of the cells are in G2/M phase (Figure 13A). The phosphorylated form of Cdk5 is also enhanced in the nucleus during G2/M phase (Figure 13B) correlating with an increase in Cdk5 activity at 12 h after synchronization (Figure 13C). These data strongly indicate an essential role of Cdk5 in the nucleus during G2/M phase. This observation was further verified by analyzing cell cycle progression of Cdk5 knockdown cells in parallel to control cells. Directly after aphidicolin release, both curves are congruent. However, at 12 h after synchronization, when the cells reach the G2/M phase there is a gap between both cell cycle curves (Figure 13D). Cdk5 knockdown cells show a higher number of cells with high PI-fluorescence. This result suggests that Cdk5 knockdown causes a delayed mitosis and therefore slower proliferation of HCC cells.

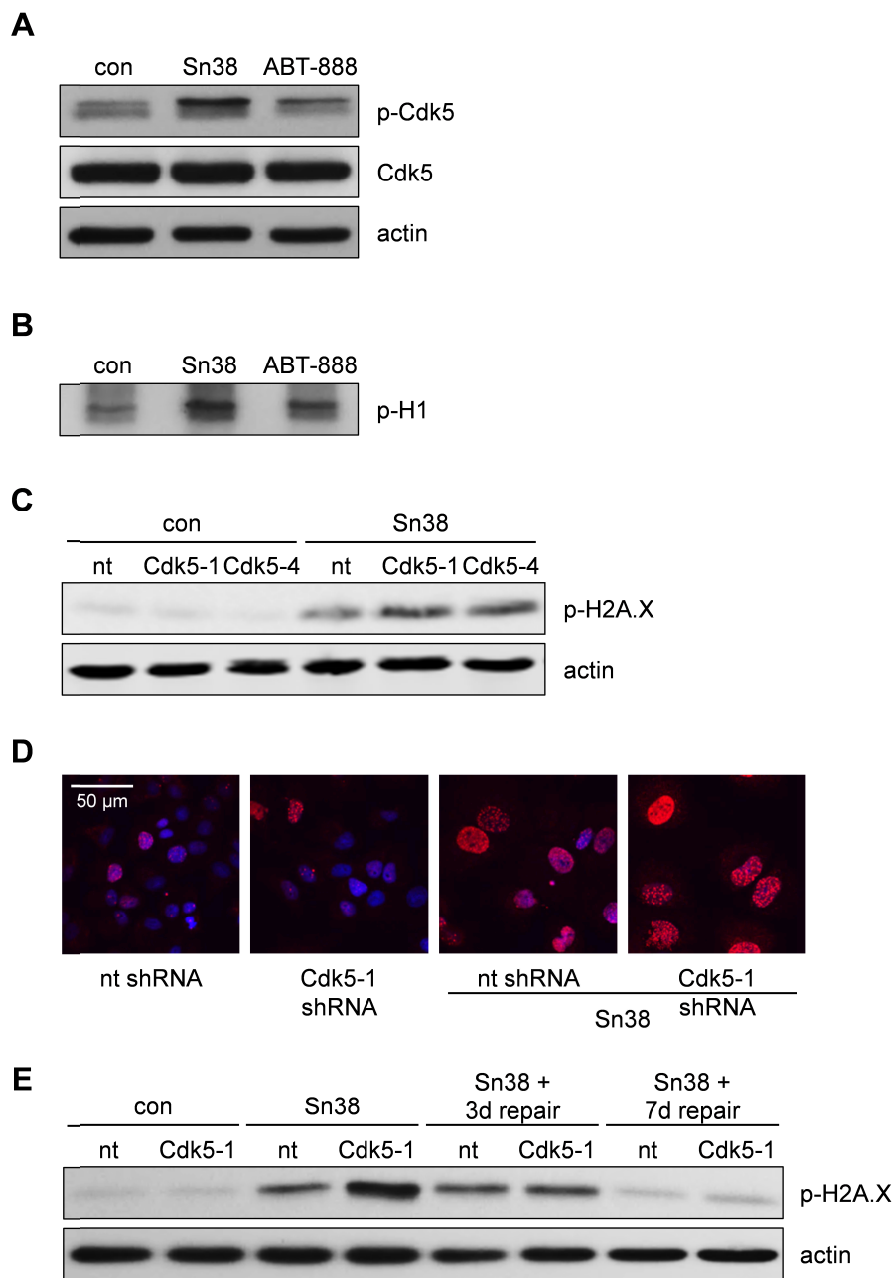




**Figure 13 Cdk5 is activated in the nucleus of HCC cells during G2/M cell cycle phase.** (A) HUH7 cells were synchronized by aphidicolin (10  $\mu$ M, 24 h) and after removal cell cycle progression was determined. (B) Nuclear and cytosolic fractions from HUH7 cells that were synchronized with aphidicolin and released for the indicated times were immunoblotted and probed with antibodies for phosphorylated Cdk5 (p-Cdk5), Cdk5, and p27. Immunoblots for CREB and tubulin indicate fractionation and loading control. (C) Radioactive kinase assays of nuclear and cytoplasmic fractions from HUH7 cells 0 h, 12 h, and 24 h after synchronization are shown. Phosphorylated (P-32) histone 1 (p-H1) indicates Cdk5 activity. (D) Nt and Cdk5 shRNA cells were synchronized by aphidicolin and after release cell cycle progression was determined by Nicoletti method.

### **3.3.3 Cdk5 gets activated by DNA damage and is involved in DNA damage response**

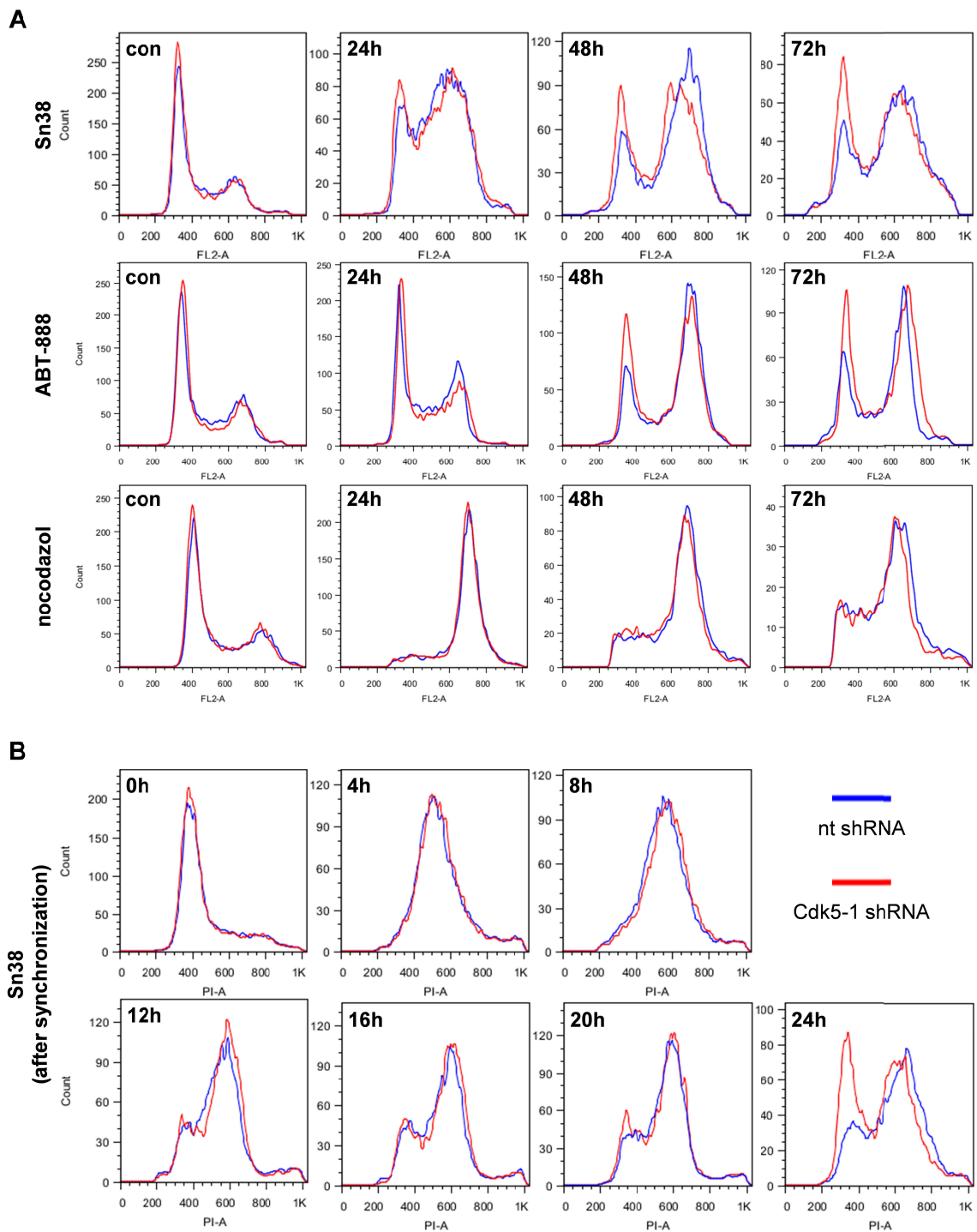
Our data demonstrated a role of Cdk5 in the nucleus during G2/M phase. During this phase DNA damage response and repair mechanism take place, which are especially important for highly proliferating cells as HCC cells. We started out to investigate whether Cdk5 affects the response of HCC cells to DNA damage inducing agents and the other way around, if DNA damaging agents affect Cdk5. With respect to the latter, we used Sn38, an active metabolite of the topoisomerase inhibitor irinotecan, as well as ABT-888, an inhibitor of PARP as DNA damage inducing chemotherapeutics. Both drugs led to an increase of phosphorylated Cdk5 (Figure 14A) and enhanced Cdk5 activity in the nucleus (Figure 14B). Importantly, cells which do not express Cdk5 responded with increased amount of DSB indicated by p-H2A.X upon Sn38 exposure in comparison to control cells (Figure 14C, D). To examine whether this increase is due to an enhanced induction or persistence of DSBs, we analyzed the p-H2A.X after removal of the DNA damage agent. Increased DSBs in Cdk5 silenced cells which occur directly after stimulation with Sn38 does not persist after removal of the DNA damaging agent (Figure 14E). Thus Cdk5 seems to be involved in the induction of DSBs rather than their persistence.



**Figure 14 Cdk5 gets activated by treatment with DNA damage agents and plays a role in the response.** (A) HUH7 cells were stimulated with Sn38 (5 ng/mL) or ABT-888 (100  $\mu$ M) for 24 h and protein levels were evaluated by Western blot. (B) With the same conditions, Cdk5 activity was measured in the nuclear fractions using radioactivity assay. (C) Nt and Cdk5 shRNA HUH7 cells were treated with Sn38 (5 ng/mL, 48 h) and DSB were detected with specific antibody for p-H2A.X. (D) Phosphorylated H2A.X foci (red) and nuclei (blue) of nt and Cdk5 shRNA HUH7 cells were visualized by immunostaining. (E) Nt and Cdk5 shRNA HUH7 cells were treated with Sn38 (5 ng/mL, 24 h). After removal, DSB were detected after 3 and 7 d. Conducted by M. Ardelt.

### 3.3.4 Cdk5 influences DNA damage checkpoint regulation

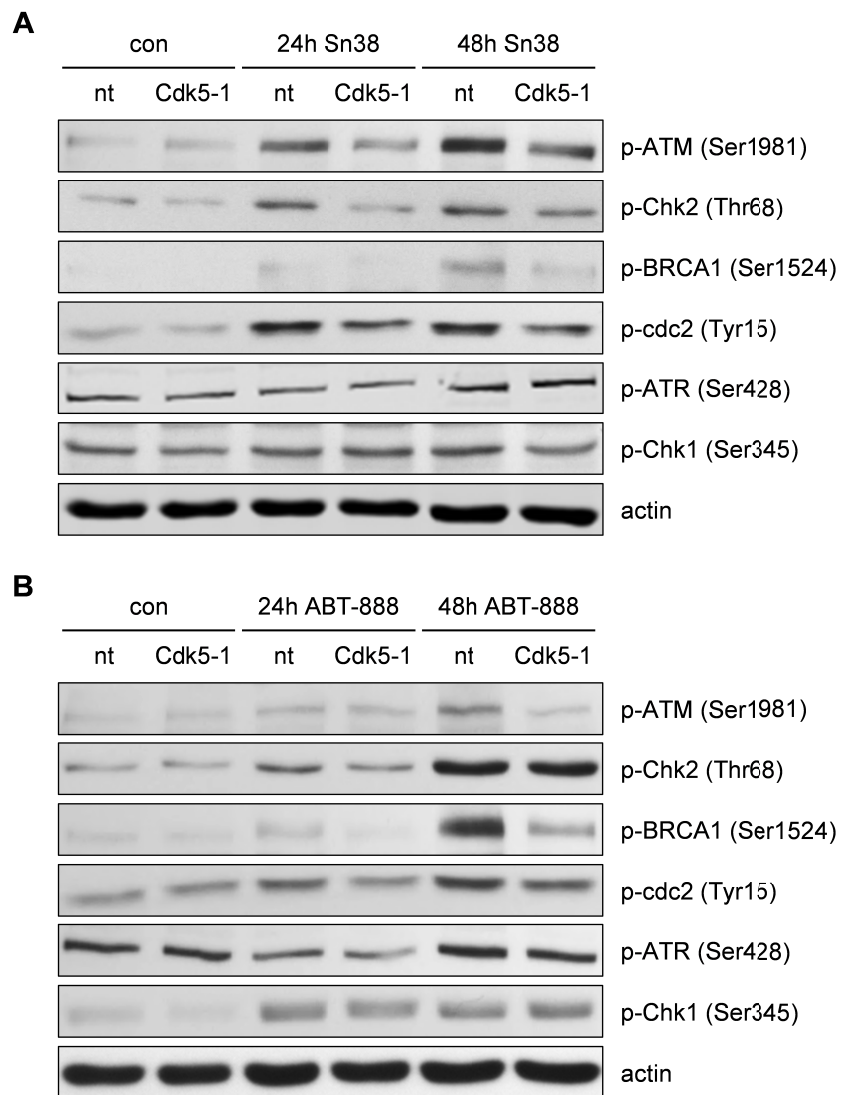
The next question was how Cdk5 knockdown causes enhanced DNA damage in HCC cells. The topoisomerase I inhibitor Sn38 causes a cell cycle arrest in the G2/M phase in control HUH7 cells (Figure 15A). Interestingly, Cdk5 shRNA cells display an increased number of cells in the G0/G1 phase upon Sn38 treatment. This effect is not restricted to Sn38 as induction of DNA damage by the PARP inhibitor ABT-888 showed the same result (Figure 15A). However, if treating the cells with nocodazol, which interferes with spindle formation rather than DNA, control as well as Cdk5 knockdown cells arrest equally in G2/M phase (Figure 15A). These results together indicate that this overcome of G2/M cell cycle arrest occurs only if it is induced by DNA damage. To illustrate whether Cdk5 knockdown cells arrest already in G0/G1 phase due to DNA damage agents and never reach the G2/M phase, or whether they overcome the G2 arrest caused by DNA damage, get into G0/G1 phase and accumulate here, we observed the cell cycle at different time points during stimulation with Sn38 after synchronizing the cells (Figure 15B). At 8 h to 12 h after synchronization and Sn38 treatment most of control as well as Cdk5 shRNA cells are in G2/M phase. Then the population of cells in G0/G1 phase increased slightly during the next 12 h in the control cells, however this population was significantly higher in Cdk5 knockdown cells. Obviously Cdk5 is important for activation of the G2/M checkpoint and loss of Cdk5 let HCC cells overcome the arrest caused by treatment with DNA damage agents. This defect in DNA damage induced checkpoint activation could be the cause for the higher amount of DSBs in Cdk5 knockdown cells as Cdk5 knockdown cells probably do not stop replicating the DNA.



**Figure 15 Cdk5 is important for DNA damage checkpoint activation.** (A) Cell cycle analysis from nt (blue) and Cdk5 (red) shRNA HUH7 cells after treatment with Sn38 (5 ng/mL), ABT-888 (100  $\mu$ M) or nocodazol (50 ng/mL) is shown. Partly conducted by M. Ardeit. (B) Cell cycle progression of nt and Cdk5 shRNA HUH7 cells was analyzed after synchronization with aphidicolin and treatment with Sn38 (5 ng/mL).

### 3.3.5 Cdk5 is important for ATM phosphorylation

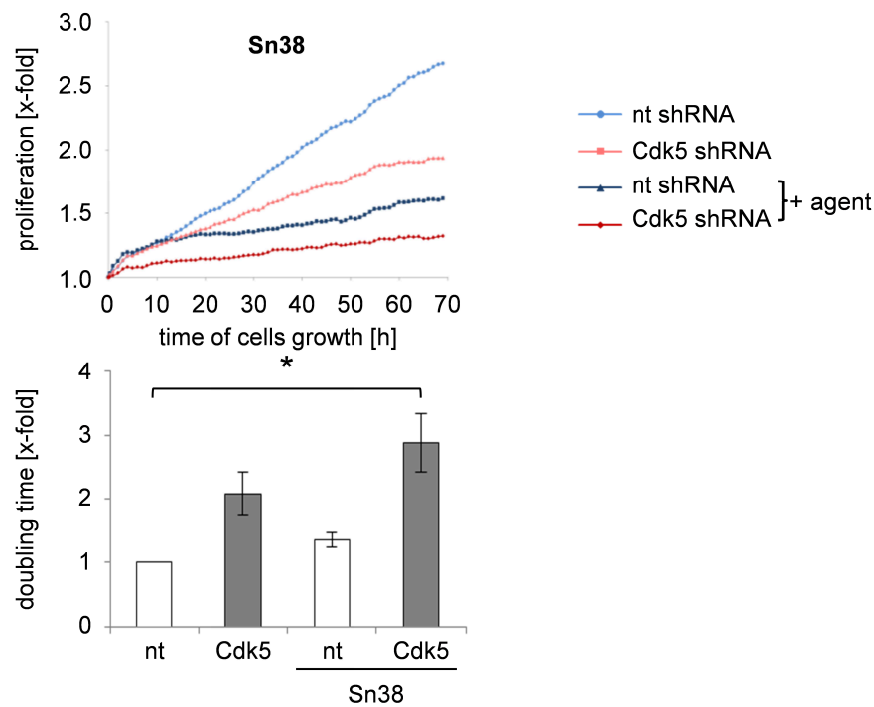
In search for the target responsible for Cdk5 induced DNA damage response and checkpoint activation the ataxia telangiectasia mutated (ATM) and ataxia telangiectasia and Rad3-related (ATR) signaling cascade gained attention. As expected, stimulation of HCC cells with Sn38 or ABT-888 led to an increase in ATM phosphorylation due to DNA damage. Interestingly, the Cdk5 knockdown cells showed a decreased phosphorylation of ATM at Ser1981, which is crucial for its activity (Figure 16A, B). However, there was no difference in phosphorylation of ATR due to Cdk5 inhibition and also its downstream target the checkpoint kinase (Chk) 1 was unaffected. In contrast, the downstream targets of ATM were influenced by Cdk5. Chk2 gets directly phosphorylated by ATM and therefore the phosphorylation at Thr68 was reduced in Cdk5 knockdown cells. In addition, the breast cancer 1 (BRCA1) protein and cyclin dependent kinase 1 (cdc2) were less phosphorylated due to Cdk5 inhibition. Thus ATM is suggested to be an important player of Cdk5 in HCC.



**Figure 16 Cdk5 is involved in ATM phosphorylation.** (A, B) Nt and Cdk5 shRNA HUH7 cells were stimulated with (A) Sn38 (5 ng/mL) or (B) ABT-888 (100  $\mu$ M) for 24 h and 48 h and analyzed with antibodies for phosphorylated ATM (p-ATM), p-Chk2, p-BRCA1, p-cdc2, p-ATR, and p-Chk1 by Western blot. Partly conducted by M. Ardelt.

### 3.4 Cdk5 inhibition chemosensitizes HCC cells for treatment with DNA damage chemotherapeutics

We showed that Cdk5 is involved in DNA damage response in HCC cells. To illustrate the therapeutic relevance we combined Cdk5 inhibition with established DNA damage inducing chemotherapeutics. The combination of DNA damage agents, like Sn38, ABT-888, doxorubicin or etoposid and inhibition of Cdk5 synergistically decreased HCC cell proliferation (Figure 17). The synergism was calculated using the Bliss formula (Values ( $v$ ) = 1.9 for Sn38,  $v$  = 2.2 for ABT-888,  $v$  = 1.1 for etoposid,  $v$  = 1.3 for doxorubicin). In contrast, nocodazol, which acts on microtubule polymerization and not on DNA damage, increases indeed the doubling time of nt and Cdk5 shRNA HUH7 cells, but there was no synergistic effect between nocodazol treatment and Cdk5 downregulation (Figure 17) ( $v$  = 1.0). These results clearly indicate that Cdk5 downregulation specifically chemosensitizes HCC cells for treatment with DNA damage inducing chemotherapeutics.



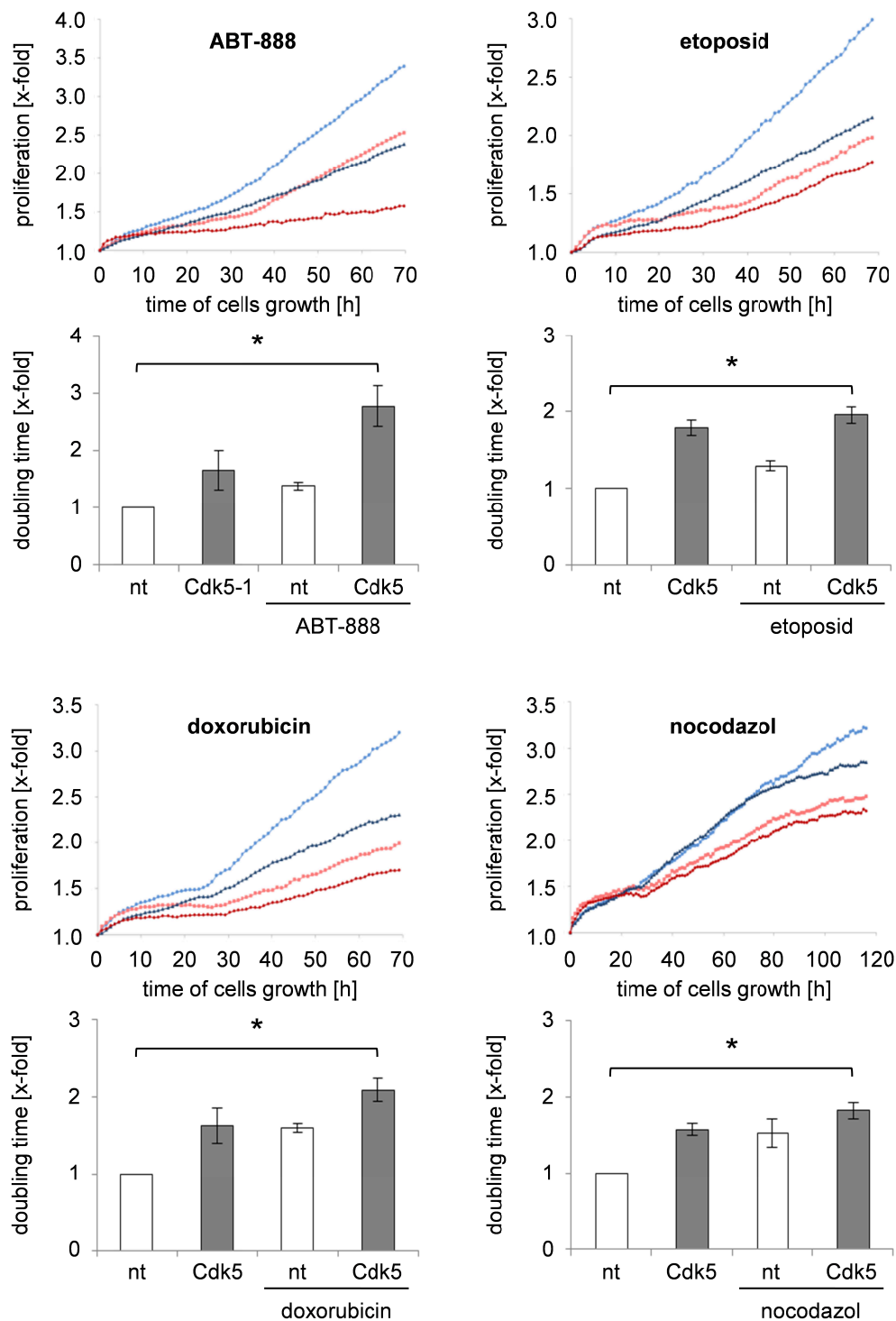


**Figure 17 Proliferation of HCC cells is synergistically inhibited by combination of Cdk5 knockdown and treatment with DNA damage agents.** Nt and Cdk5 shRNA HUH7 cells were synchronized and subsequently treated with Sn38 (1 ng/mL), ABT-888 (10  $\mu$ M), etoposid (0.1  $\mu$ M), doxorubicin (5 nM), and nocodazol (10 ng/mL). Cell growth was analyzed by xCELLigence technology. Representative curves and combined corresponding doubling times are shown. (Sn38, doxorubicin and nocodazol: One Way ANOVA, Holm-Sidak  $*p < 0.05$ ,  $n = 3$ ). (ABT-888 and etoposid: One Way ANOVA on Ranks, Dunn's  $*p < 0.05$ ,  $n = 3$ ). Partly conducted by M. Ardel.

This combined therapy reduces HCC cell proliferation directly from the beginning of treatment. In hospital routines, chemotherapy treatment is given in cycles to attack cancer cells most effectively, whereas the body's normal cells have time to recover in between. To get closer to this patient situation, we further tested the combinatorial treatments in clonogenic survival assays (Figure 18A). Remarkably, stimulation with all tested DNA damage agents and Cdk5 downregulation decrease significantly colony formation ability of HCC cells. The profound effect is due to the combined effects of decreased proliferation and enhanced apoptosis in Cdk5 knockdown cells 7 days after short-term stimulation (Figure 18B). Moreover, these *in vitro* results could be verified *in vivo*, as the combined systemic treatment of the Cdk5 inhibitor roscovitine and irinotecan, the therapeutically used prodrug of Sn38, increased inhibition of tumor growth in a HCC xenograft model (Figure 18C).

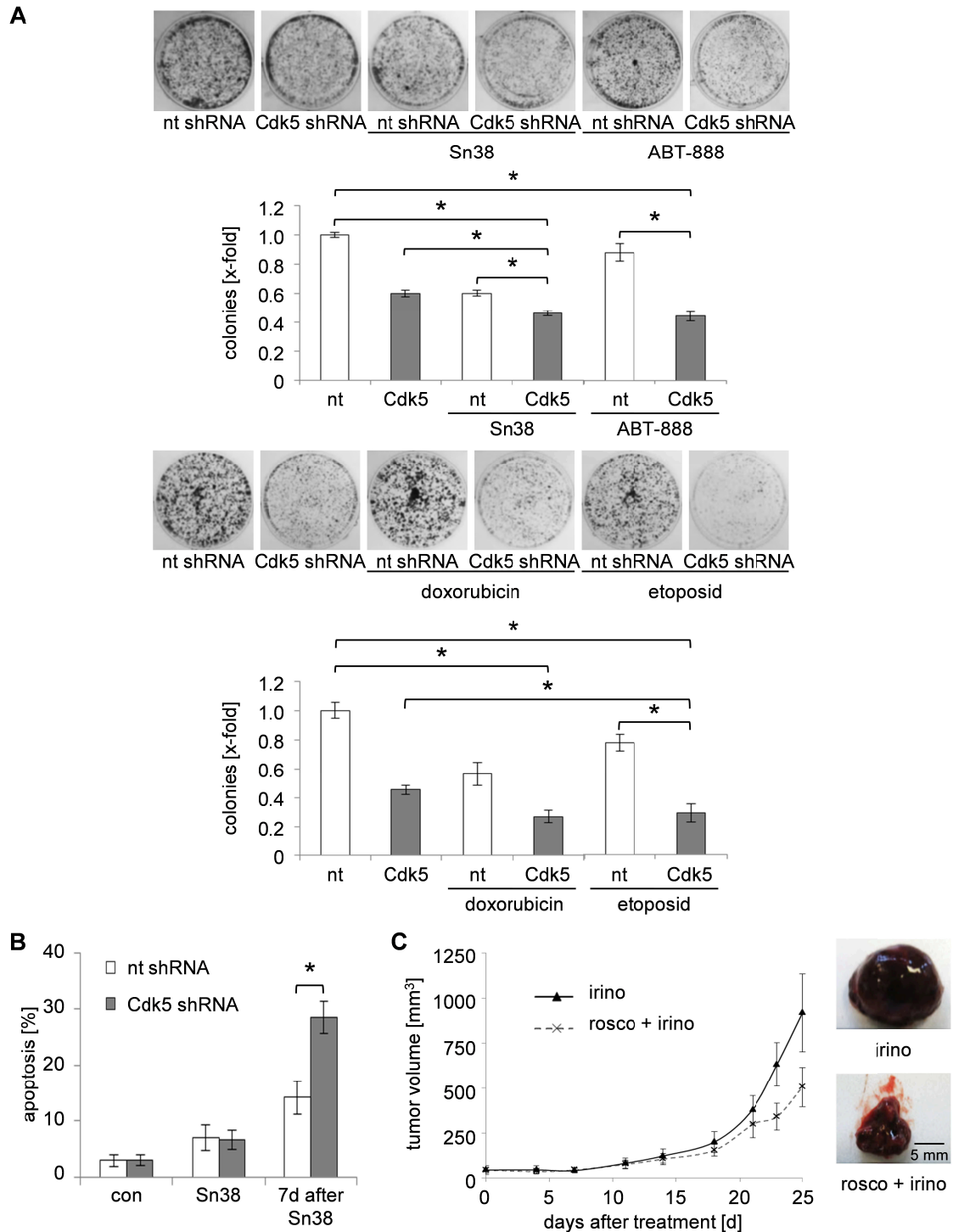


**Figure 18 Cdk5 inhibition sensitizes HCC cells for treatment with DNA damage agents *in vitro* and *in vivo*.** (A) Colony formation of nt and Cdk5 shRNA HUH7 cells treated with Sn38 (1 ng/mL), ABT-888 (10  $\mu$ M), etoposid (0.1  $\mu$ M), and doxorubicin (5 nM) for 24 h is shown. (Sn38 and etoposid: One Way ANOVA, Holm-Sidak  $*p < 0.05$ ,  $n = 3$ ). (ABT-888 and doxorubicin: One Way ANOVA on Ranks, Dunn's  $*p < 0.05$ ,  $n = 3$ ). (B) Nt and Cdk5 shRNA HUH7 cells were treated with Sn38 (5 ng/mL, 48 h). After removal of Sn38, apoptotic cells were detected after additional 7 d using flow cytometry. (One Way ANOVA, Holm-Sidak  $*p < 0.05$ ,  $n = 3$ ). Conducted by M. Ardelit. (C) Tumors of HUH7 cells grown in SCID mice that were treated with irinotecan or a combination of roscovitine and irinotecan are shown (irino:  $n = 5$ , combination:  $n = 7$ ). Tumor volume was monitored over time after finishing the treatment.

### 3.5 Cdk5 inhibition enhances efficacy of sorafenib treatment in HCC cells

#### 3.5.1 Cdk5 inhibition acts synergistic with sorafenib on HCC tumor growth

The only approved systemic treatment option for advanced HCC is sorafenib. However its therapeutic success is limited with a survival advantage of 2-3 months and a response rate of 2%.<sup>7</sup> Therefore, it is of paramount clinical importance to enhance the efficacy of sorafenib treatment. Our hypothesis was that combination of sorafenib with Cdk5 inhibition has a beneficial effect on HCC growth inhibition. In fact, clonogenic survival and proliferation (Bliss Value = 2.0) of HCC cells is synergistically reduced by the combined treatment of sorafenib and Cdk5 downregulation (Figure 19A, B).

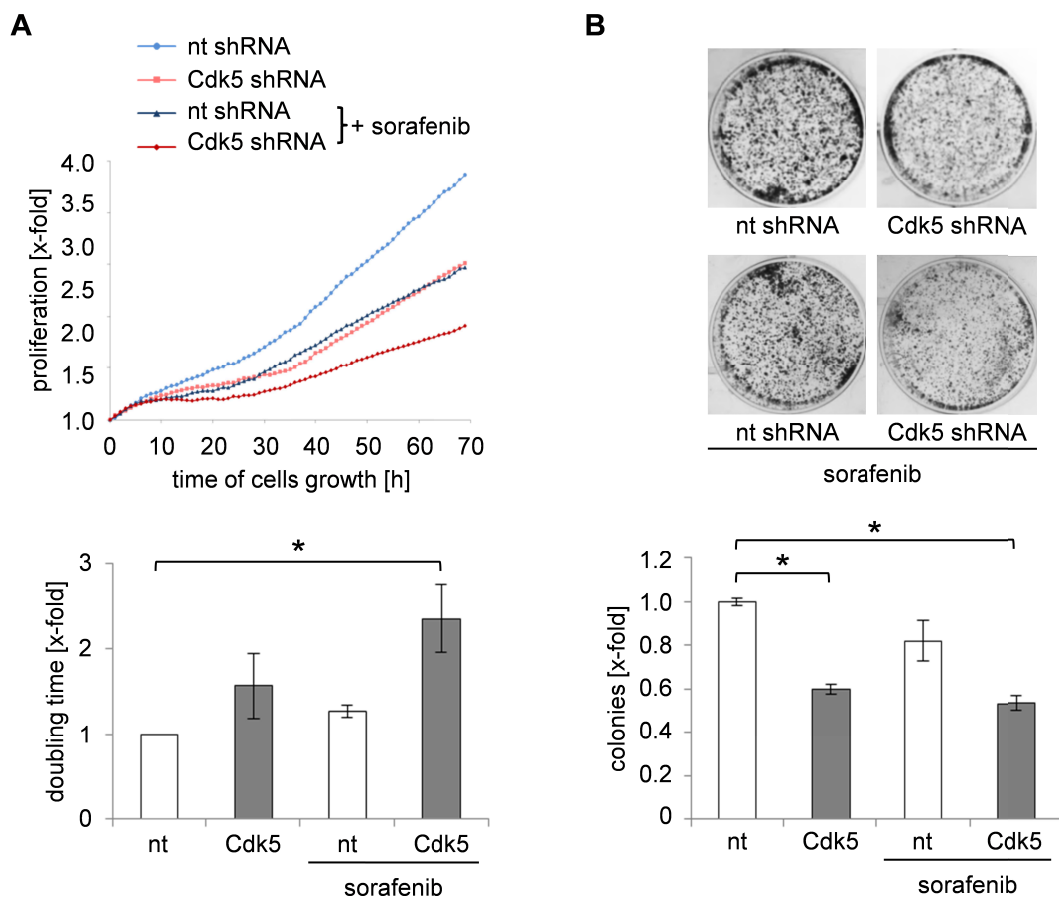


**Figure 19 Cdk5 knockdown sensitizes HCC cells for treatment with sorafenib.** (A) Nt and Cdk5 shRNA HUH7 cells were synchronized by aphidicolin and treated with sorafenib (4  $\mu$ M). Cell growth was analyzed by xCELLigence. Representative curves and combined corresponding doubling times are shown. (One Way ANOVA on Ranks, Dunn's  $*p < 0.05$ ,  $n = 3$ ). Conducted by M. Ardelt. (B) Colony formation of nt and Cdk5 shRNA HUH7 cells treated with sorafenib (4  $\mu$ M) for 24 h is shown. (One Way ANOVA on Ranks, Dunn's  $*p < 0.05$ ,  $n = 3$ ).

### 3.5.2 Inhibition of Cdk5 prevents the cell migration induced by low-dose sorafenib

Moreover, we investigated the effects of combining Cdk5 knockdown with sorafenib treatment on HCC cell migration. Transwell migration assays revealed that low doses of sorafenib (0.5  $\mu$ M) significantly increased cell migration (Figure 20). Interestingly, Cdk5 knockdown suppressed the sorafenib-induced cell migration (Figure 20).

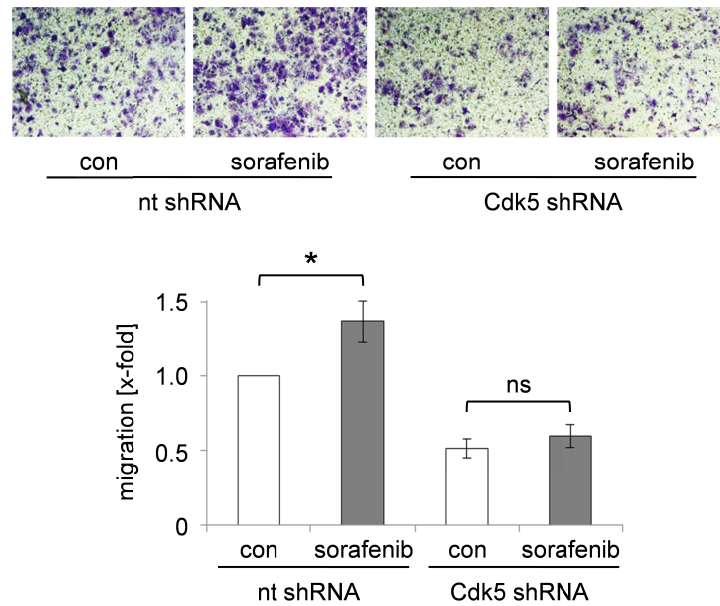


**Figure 20 Cdk5 knockdown reduces HCC cell migration induced by sorafenib.** Transwell migration of nt and Cdk5 shRNA HUH7 cells pretreated with sorafenib (0.5  $\mu$ M, 24 h) was determined by Boyden Chamber assays. The graph displays the number of migrated cells related to control. (One Way ANOVA on Ranks, Student-Newman-Keuls  $*p < 0.05$ ,  $n = 3$ ). Conducted by M. Ardelt.

## **DISCUSSION**

## 4 DISCUSSION

Prognosis for patients with advanced stage HCC, *i.e.* when curative surgery is no longer feasible, is very poor. Up to now, oral treatment with the multi tyrosine kinase inhibitor sorafenib represents the only approved systemic therapeutic option for advanced stage HCC.<sup>6</sup> However, its therapeutic success is limited, because response remains low and the median overall survival is only extended by 2-3 months.<sup>7</sup> This urgently demands for new systemic treatment strategies for HCC therapy.

### 4.1 Cdk5 is an important mediator in HCC progression

Our present study provides evidence for Cdk5 as a novel target for HCC therapy. In fact, we demonstrate for the first time a crucial role of Cdk5 in HCC progression and thereby extend the rare knowledge of Cdk5 in cancer. Increased expression of Cdk5 and p35 in HCC tissue in comparison to healthy liver tissue goes along with pancreatic cancer<sup>49</sup> and non-small cell lung cancer, where high expression of Cdk5/p35 is related to poor patient prognosis.<sup>50</sup>

Moreover in our study, we showed that genetic and pharmacologic inhibition of Cdk5 decreases significantly HCC cell motility and invasion. Remarkably, Cdk5 controls proliferation of HCC cells and inhibits tumor growth *in vivo*. These findings are partly in line with the few publications about Cdk5 in other cancer types, but also reveal a specific functional profile and signaling of Cdk5 in HCC. In prostate cancer, Cdk5 regulates cell motility and metastatic potential,<sup>36</sup> but has no influence on tumor growth, whereas in pancreatic cancer, similar to HCC, Cdk5 is involved in the whole tumor progression including cell proliferation and motility.<sup>37</sup> In pancreatic cancer, Cdk5 acts *via* activation of Ral effector pathway which is essential for oncogenic Ras signaling.<sup>37</sup> Furthermore, dysregulated high activity of Cdk5 in C cells of the thyroid gland was reported to initiate the formation of medullary thyroid carcinoma *via* phosphorylation of retinoblastoma protein.<sup>34</sup> Regarding the fact that Cdk5 affects cancer genesis as shown in neuroendocrine thyroid cancer it might be reasonable to study the role of Cdk5 in HCC onset mostly driven by liver cirrhosis and hepatitis infection in future projects.

## 4.2 Cdk5 regulates DNA damage response and checkpoint activation *via* ATM pathway

Our results imply a Cdk5 driven signaling which is so far unique and novel in HCC. We suggest ATM signaling as Cdk5 downstream pathway responsible for its synergistic effects with DNA damage agents in HCC.

The ATM and ATR signaling cascade is the major response to DNA damage and acts thereby on different axes: it regulates cell cycle arrest, activates DNA repair mechanisms, and induces cell death.<sup>51</sup> ATM acts as sensor for the DNA damage and as transducer for the response. In the role of the latter, ATM activates several proteins, like BRCA1, which is involved in DNA damage repair,<sup>52</sup> the checkpoint kinase 2 (Chk2) and p53. P53 can be directly phosphorylated by ATM or indirect *via* Chk2. The activated p53, in turn, can trigger cells to apoptosis or to cell cycle arrest in the G1 phase.<sup>51</sup> ATR is another protein with a role as transducer in response to DNA damage. As ATR shares high sequence homology to ATM, there is a high degree of redundancy in the DNA damage response pathways. However, in general, Chk1 is preferentially phosphorylated by ATR, while Chk2 is the favored ATM substrate.<sup>53</sup> Different isoforms of the Cdc25 phosphatase are the important key targets of Chk1 and Chk2. Cdc25A regulates progression through S phase, and Cdc25B and Cdc25C control mitotic entry.<sup>54</sup> The phosphorylation by Chk1 and Chk2 causes an inactivation of Cdc25 phosphatase. Thus, the ATR/ATM-Chk1/Chk2-Cdc25 pathways regulate the G1/S and G2/M checkpoints, respectively (Figure 21).

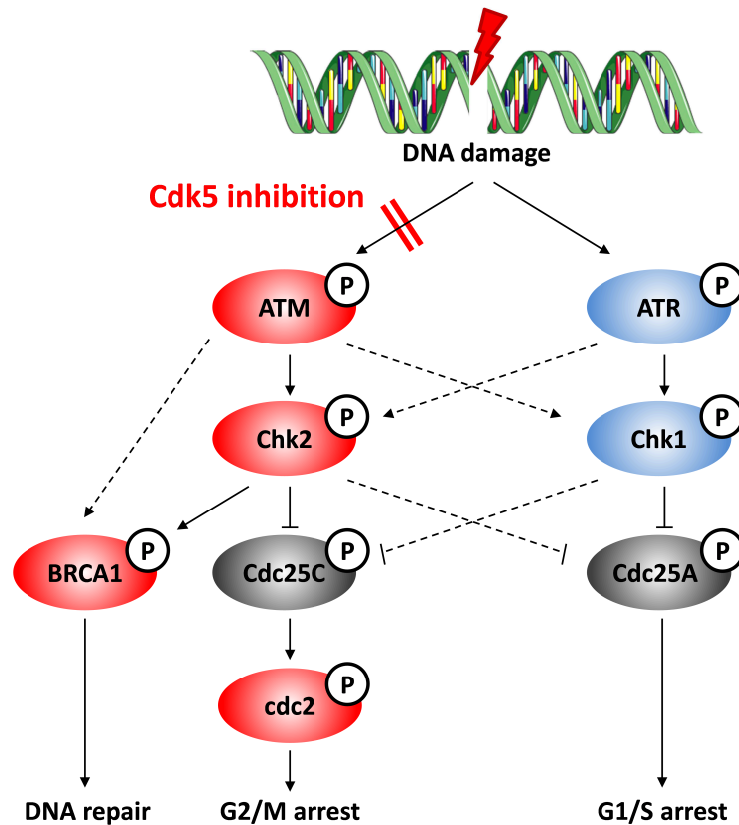


**Figure 21 ATM/ATR signaling pathway in DNA damage response and cell cycle checkpoint regulation.** Cdk5 affects phosphorylation of ATM, Chk2, BRCA1 and cdc2 (red), but has no influence on ATR and Chk1 (blue). Details can be found in the text.

Whereas the ATR pathway is not affected, we showed that ATM is influenced by Cdk5. Cdk5 inhibition results in reduced ATM autophosphorylation at Ser1981, which is essential for its activity. In the following, Cdk5 affects the whole signaling pathway downstream of ATM including Chk2, BRCA1 and cdc2 phosphorylation, suggesting that Cdk5 thereby regulates DSB induction and G2/M checkpoint activation.

Neuronal Cdk5 directly phosphorylates ATM at Ser794 and thereby triggers the autophosphorylation at Ser1981. Nevertheless, in neurons less ATM phosphorylation due to Cdk5 inhibition leads to reduced induction of DSBs and resulted in prevention from neuronal death.<sup>55</sup> However, in contrast, Cdk5 inhibition in HCC cells increases DSB formation induced by DNA damaging agents. This different response to less ATM phosphorylation might be due to basal difference between postmitotic neurons and highly proliferating HCC cells. Due to the postmitotic status, the regulation of cell cycle in neurons differs from proliferating cells as e.g. the onset of cell cycle in adult neurons leads to cell death.<sup>56, 57</sup> Moreover, function of Cdk5 varies also in other cases concerning cell proliferation between neurons and cancer cells: In neurons, Cdk5 suppresses the initiation

of cell cycle, if located in the nucleus,<sup>48</sup> whereas in HCC we showed that only cells with Cdk5 located in the nucleus are positive for the proliferation marker Ki-67. Along this line, one could suggest that function and regulation of Cdk5 in HCC are in parallel to neurons, i.e. ATM might be a direct target, but this cannot be transferred without further evaluation.

In addition, we showed that Cdk5 inhibition enhances the response of HCC cells to different DNA damaging agents, including topoisomerase inhibitors irinotecan, etoposid and doxorubicin, and the PARP inhibitor ABT-888. Our data are in line with studies in other cancer types, where an involvement of Cdk5 in DNA damage response has been shown.<sup>58, 59</sup> However, up to now the ATM signaling is not well investigated in HCC. Thus, our results represent an important step in introducing Cdk5 and the ATM pathway as possible target for HCC therapy.

### **4.3 Combination of Cdk5 inhibition with DNA damage agents presents a novel therapeutic option for HCC**

Our clinical most important finding showed that combination of Cdk5 inhibition with different DNA damage inducing chemotherapeutics synergistically inhibits HCC tumor progression by decreasing cell growth and inducing cell death. These results suggested novel and promising therapeutic strategies for therapy of patients with advanced stage HCC. We tested different DNA damage agents, like irinotecan, ABT-888, etoposid and doxorubicin, for the combined treatment with Cdk5 inhibition.

The PARP inhibitor ABT-888 is up to now mostly studied in preclinical models of different cancer types, like glioblastoma, colorectal cancer and prostate cancer.<sup>60-62</sup> Some publications show also a synergistic effect of ABT-888 with DNA damage induction by chemotherapeutics or radiation.<sup>63, 64</sup> Our study indicates a benefit of combining this PARP inhibitor with Cdk5 inhibition. A combination of Cdk5 inhibition with PARP inhibition and DNA damage induction for treatment of HCC patients could represent an additional option.

Doxorubicin is given for treatment of HCC mostly *via* TACE.<sup>65</sup> In some case reports doxorubicin is also applied systemically, but the response rate is only 2-10%.<sup>66, 67</sup> The combination of doxorubicin with cisplatin, interferon and fluorouracil enhances the response rate to 20%. However, this is associated with significant toxicity including two treatment related deaths.<sup>68</sup>

Irinotecan is well-established as single as well as combination approaches in treatment of other cancer types like e.g. metastatic colorectal cancer.<sup>69</sup> Importantly, few single case reports show a response of HCC patients to irinotecan.<sup>70-72</sup> Although potentially effective, high dose chemotherapy with irinotecan leads to gastrointestinal and vascular side effects, which clearly limits the therapeutic success.<sup>73</sup>

Of note, by combining the DNA damage inducing chemotherapeutics with Cdk5 inhibitors, as proposed here, the dose can be reduced. This might diminish the problem of high toxicity due to the DNA damage agents, as Cdk5 inhibition appears to be well tolerated without the typical side effects associated with chemotherapy.<sup>74</sup>

In summary we introduced these chemotherapeutics in combination with Cdk5 inhibition as new therapeutic strategies.

#### **4.4 Cdk5 inhibition increases efficacy and response to sorafenib treatment**

Up to now, sorafenib is the standard first-line systemic drug for treatment of advanced HCC. However, its therapeutic benefit is limited, because the overall survival is only extended by 2-3 months and due to resistance the response remains low.<sup>7</sup> In our work, we showed that the efficacy of sorafenib treatment can be enhanced by combination with Cdk5 inhibition as combined therapy inhibits synergistically HCC tumor growth and prevents sorafenib induced HCC cell migration.

Sorafenib inhibits a variety of different tyrosine kinases including vascular endothelial growth factor receptor (VEGFR-) 1, VEGFR-2, VEGFR-3, platelet-derived growth factor receptor (PDGFR-)  $\beta$ , RET, c-KIT, FMS-like tyrosine kinase-3, and also the RAF/mitogen-activated protein kinase (MAPK)/extracellular signaling-regulated kinase (ERK) pathway by targeting Raf-1 and B-Raf.<sup>75, 76</sup> The phosphatidylinositol 3-kinase (PI3K)/Akt and the MAPK signaling pathways are most important for HCC progression. While the MAPK pathway is inhibited by sorafenib, it is reported that Akt is activated by sorafenib as a compensatory mechanism. In addition, the resistance to sorafenib could be reversed by Akt inhibition, suggesting that the Akt pathway is involved in sorafenib resistance.<sup>77-79</sup> Fujimaki *et al.* suggest that the sorafenib mediated Akt phosphorylation occurs *via* ATM activation.<sup>77</sup> As our findings already showed that Cdk5 inhibition prevents ATM and Akt phosphorylation, this could be the mechanistical explanation for the synergistic effect of

combining sorafenib with Cdk5 inhibition. This combination is a new therapeutic approach to enhance sorafenib treatment response and efficacy.

#### 4.5 Cdk5 represents a novel drugable target for HCC therapy

One of the earliest and most popular Cdk5 inhibitors is roscovitine. However, it is far from selectively inhibiting Cdk5 as it also targets Cdk1, Cdk2, Cdk7, Cdk9, ERK1/2 and pyridoxal kinase.<sup>39, 40</sup> During last years, many groups tried to develop new Cdk5 inhibitors with improved potency and selectivity using roscovitine as mother substance<sup>80-82</sup> and also other lead structures, e.g. Dinaciclib (SCH 727965).<sup>83-85</sup> Most of these compounds show an increased potency for Cdk5 inhibition, but they still share the problem of selectivity as they target at least also Cdk1 and Cdk2. This selectivity problem occurs due to their interaction with the ATP-binding pocket which is quite conserved throughout the Cdk family. A new approach is the inhibition of the interaction of Cdk5 and its activators.<sup>86, 87</sup> These inhibitors mainly target the interaction of Cdk5 and p25, the truncated form of p35, which is associated with a dysregulated activity of Cdk5 and therefore with pathogenesis of neurodegenerative diseases. Zeng *et al.* reported that a short peptide called CIP (Cdk5 inhibitory peptide), which is derived from p35, specifically inhibits the Cdk5/p25 activity, without affecting the activity of Cdk1 or Cdk5/p35.<sup>88, 89</sup> Thus, targeting the interaction of Cdk5 and its activators represents a promising option for developing selective Cdk5 inhibitors. However, to use this approach in HCC, it is important to elucidate first if Cdk5 activity in HCC depends also on binding to p35 and p25, like in neurons, or on different proteins.

#### 4.6 Conclusion and further perspectives

In conclusion, this study for the first time presents a novel and crucial function of Cdk5 in HCC cell motility and tumor growth. We showed that inhibition of Cdk5 potentiates the antitumor effects of different DNA damage agents and sorafenib in hepatoma cells and suggested a specific signaling pathway for these effects. Our work demonstrate Cdk5 as a drugable target in HCC and proposes the combination of DNA damage inducing chemotherapeutics or sorafenib and Cdk5 inhibition as a novel and promising therapeutic strategy for this almost lethal disease.

## **SUMMARY**

## 5 SUMMARY

For a long time cyclin dependent kinase 5 (Cdk5) was thought to be of exclusive importance in neuronal cells. However, recently increasing evidence suggests a function of Cdk5 in cancer progression. In the present study, we examined the role of Cdk5 in hepatocellular carcinoma (HCC), a highly chemoresistant cancer with poor prognosis. Consequently, development of novel targeted therapies for HCC is of paramount clinical importance. Analysis of human HCC patient samples showed an increased expression of Cdk5 as compared to normal liver tissues. Functional ablation of Cdk5 significantly decreases HCC cell proliferation and clonogenic survival, and reduces cell motility and invasion. Of note, genetic as well as pharmacologic inhibition of Cdk5 also shows *in vivo* efficacy in a HCC xenograft mouse model. Investigating the mechanism behind these functional effects revealed that Cdk5 is most active in the nucleus of cells in G2/M phase. In this cell cycle phase DNA damage response takes place, which is affected by Cdk5 inhibition. Furthermore, Cdk5 leads to phosphorylation of Ataxia Telangiectasia Mutated (ATM) and thereby influence its downstream signaling. Importantly, combination of Cdk5 inhibition with different DNA damage inducing chemotherapeutics or the first-line systemic drug sorafenib inhibits synergistically HCC tumor progression.

**In conclusion, we introduce:**

1. Cdk5 as a novel drugable target for treatment of HCC
2. The combination of Cdk5 inhibition and DNA damage agents as a novel therapeutic approach
3. An increased efficacy of sorafenib treatment by combing with Cdk5 inhibition

## REFERENCES

## 6 REFERENCES

1. El-Serag HB. Hepatocellular carcinoma. *N Engl J Med* 2011;365:1118-1127.
2. Jemal A, Bray F, Center MM, Ferlay J, Ward E, Forman D. Global cancer statistics. *CA Cancer J Clin* 2011;61:69-90.
3. Lin S, Hoffmann K, Schemmer P. Treatment of Hepatocellular Carcinoma: A Systematic Review. *Liver Cancer* 2012;1:144-158.
4. El-Serag HB, Marrero JA, Rudolph L, Reddy KR. Diagnosis and treatment of hepatocellular carcinoma. *Gastroenterology* 2008;134:1752-1763.
5. Davila JA, Duan Z, McGlynn KA, El-Serag HB. Utilization and outcomes of palliative therapy for hepatocellular carcinoma: a population-based study in the United States. *J Clin Gastroenterol* 2012;46:71-77.
6. Bruix J, Sherman M, American Association for the Study of Liver D. Management of hepatocellular carcinoma: an update. *Hepatology* 2011;53:1020-1022.
7. Llovet JM, Ricci S, Mazzaferro V, Hilgard P, Gane E, Blanc JF, de Oliveira AC, et al. Sorafenib in advanced hepatocellular carcinoma. *N Engl J Med* 2008;359:378-390.
8. Lew J, Beaudette K, Litwin CM, Wang JH. Purification and characterization of a novel proline-directed protein kinase from bovine brain. *J Biol Chem* 1992;267:13383-13390.
9. Dhavan R, Tsai LH. A decade of CDK5. *Nat Rev Mol Cell Biol* 2001;2:749-759.
10. Liebl J, Furst R, Vollmar AM, Zahler S. Twice switched at birth: cell cycle-independent roles of the "neuron-specific" cyclin-dependent kinase 5 (Cdk5) in non-neuronal cells. *Cell Signal* 2011;23:1698-1707.
11. Humbert S, Dhavan R, Tsai L. p39 activates cdk5 in neurons, and is associated with the actin cytoskeleton. *J Cell Sci* 2000;113 ( Pt 6):975-983.
12. Tsai LH, Delalle I, Caviness VS, Jr., Chae T, Harlow E. p35 is a neural-specific regulatory subunit of cyclin-dependent kinase 5. *Nature* 1994;371:419-423.
13. Tang D, Yeung J, Lee KY, Matsushita M, Matsui H, Tomizawa K, Hatase O, et al. An isoform of the neuronal cyclin-dependent kinase 5 (Cdk5) activator. *J Biol Chem* 1995;270:26897-26903.
14. Ko J, Humbert S, Bronson RT, Takahashi S, Kulkarni AB, Li E, Tsai LH. p35 and p39 are essential for cyclin-dependent kinase 5 function during neurodevelopment. *J Neurosci* 2001;21:6758-6771.
15. Hisanaga S, Saito T. The regulation of cyclin-dependent kinase 5 activity through the metabolism of p35 or p39 Cdk5 activator. *Neurosignals* 2003;12:221-229.
16. Zukerberg LR, Patrick GN, Nikolic M, Humbert S, Wu CL, Lanier LM, Gertler FB, et al. Cables links Cdk5 and c-Abl and facilitates Cdk5 tyrosine phosphorylation, kinase upregulation, and neurite outgrowth. *Neuron* 2000;26:633-646.

17. Sasaki Y, Cheng C, Uchida Y, Nakajima O, Ohshima T, Yagi T, Taniguchi M, et al. Fyn and Cdk5 mediate semaphorin-3A signaling, which is involved in regulation of dendrite orientation in cerebral cortex. *Neuron* 2002;35:907-920.
18. Kobayashi H, Saito T, Sato K, Furusawa K, Hosokawa T, Tsutsumi K, Asada A, et al. Phosphorylation of Cdk5 at Tyr15 is inhibited by Cdk5 activators and does not contribute to the activation of Cdk5. *J Biol Chem* 2014.
19. Gilmore EC, Ohshima T, Goffinet AM, Kulkarni AB, Herrup K. Cyclin-dependent kinase 5-deficient mice demonstrate novel developmental arrest in cerebral cortex. *J Neurosci* 1998;18:6370-6377.
20. Ohshima T, Gilmore EC, Longenecker G, Jacobowitz DM, Brady RO, Herrup K, Kulkarni AB. Migration defects of *cdk5(-/-)* neurons in the developing cerebellum is cell autonomous. *J Neurosci* 1999;19:6017-6026.
21. Ohshima T, Ward JM, Huh CG, Longenecker G, Veeranna, Pant HC, Brady RO, et al. Targeted disruption of the cyclin-dependent kinase 5 gene results in abnormal corticogenesis, neuronal pathology and perinatal death. *Proc Natl Acad Sci U S A* 1996;93:11173-11178.
22. Hawasli AH, Benavides DR, Nguyen C, Kansy JW, Hayashi K, Chambon P, Greengard P, et al. Cyclin-dependent kinase 5 governs learning and synaptic plasticity via control of NMDAR degradation. *Nat Neurosci* 2007;10:880-886.
23. Takahashi S, Ohshima T, Cho A, Sreenath T, Iadarola MJ, Pant HC, Kim Y, et al. Increased activity of cyclin-dependent kinase 5 leads to attenuation of cocaine-mediated dopamine signaling. *Proc Natl Acad Sci U S A* 2005;102:1737-1742.
24. Noble W, Olm V, Takata K, Casey E, Mary O, Meyerson J, Gaynor K, et al. Cdk5 is a key factor in tau aggregation and tangle formation *in vivo*. *Neuron* 2003;38:555-565.
25. Tsai LH, Lee MS, Cruz J. Cdk5, a therapeutic target for Alzheimer's disease? *Biochim Biophys Acta* 2004;1697:137-142.
26. Lee MS, Kwon YT, Li M, Peng J, Friedlander RM, Tsai LH. Neurotoxicity induces cleavage of p35 to p25 by calpain. *Nature* 2000;405:360-364.
27. Patrick GN, Zukerberg L, Nikolic M, de la Monte S, Dikkes P, Tsai LH. Conversion of p35 to p25 deregulates Cdk5 activity and promotes neurodegeneration. *Nature* 1999;402:615-622.
28. Liebl J, Weitensteiner SB, Vereb G, Takacs L, Furst R, Vollmar AM, Zahler S. Cyclin-dependent kinase 5 regulates endothelial cell migration and angiogenesis. *J Biol Chem* 2010;285:35932-35943.
29. Rosales JL, Lee KY. Extraneuronal roles of cyclin-dependent kinase 5. *Bioessays* 2006;28:1023-1034.
30. Gao C, Negash S, Wang HS, Ledee D, Guo H, Russell P, Zelenka P. Cdk5 mediates changes in morphology and promotes apoptosis of astrocytoma cells in response to heat shock. *J Cell Sci* 2001;114:1145-1153.
31. Goodyear S, Sharma MC. Roscovitine regulates invasive breast cancer cell (MDA-MB231) proliferation and survival through cell cycle regulatory protein cdk5. *Exp Mol Pathol* 2007;82:25-32.

32. Lin H, Chen MC, Chiu CY, Song YM, Lin SY. Cdk5 regulates STAT3 activation and cell proliferation in medullary thyroid carcinoma cells. *J Biol Chem* 2007;282:2776-2784.
33. Liu R, Tian B, Gearing M, Hunter S, Ye K, Mao Z. Cdk5-mediated regulation of the PIKE-A-Akt pathway and glioblastoma cell invasion. *Proc Natl Acad Sci U S A* 2008;105:7570-7575.
34. Pozo K, Castro-Rivera E, Tan C, Plattner F, Schwach G, Siegl V, Meyer D, et al. The role of Cdk5 in neuroendocrine thyroid cancer. *Cancer Cell* 2013;24:499-511.
35. Sandal T, Stapnes C, Kleivdal H, Hedin L, Doskeland SO. A novel, extraneuronal role for cyclin-dependent protein kinase 5 (CDK5): modulation of cAMP-induced apoptosis in rat leukemia cells. *J Biol Chem* 2002;277:20783-20793.
36. Strock CJ, Park JI, Nakakura EK, Bova GS, Isaacs JT, Ball DW, Nelkin BD. Cyclin-dependent kinase 5 activity controls cell motility and metastatic potential of prostate cancer cells. *Cancer Res* 2006;66:7509-7515.
37. Feldmann G, Mishra A, Hong SM, Bisht S, Strock CJ, Ball DW, Goggins M, et al. Inhibiting the cyclin-dependent kinase CDK5 blocks pancreatic cancer formation and progression through the suppression of Ras-Ral signaling. *Cancer Res* 2010;70:4460-4469.
38. Vesely J, Havlicek L, Strnad M, Blow JJ, Donella-Deana A, Pinna L, Letham DS, et al. Inhibition of cyclin-dependent kinases by purine analogues. *Eur J Biochem* 1994;224:771-786.
39. Meijer L, Borgne A, Mulner O, Chong JP, Blow JJ, Inagaki N, Inagaki M, et al. Biochemical and cellular effects of roscovitine, a potent and selective inhibitor of the cyclin-dependent kinases cdc2, cdk2 and cdk5. *Eur J Biochem* 1997;243:527-536.
40. Bach S, Knockaert M, Reinhardt J, Lozach O, Schmitt S, Baratte B, Koken M, et al. Roscovitine targets, protein kinases and pyridoxal kinase. *J Biol Chem* 2005;280:31208-31219.
41. Knockaert M, Greengard P, Meijer L. Pharmacological inhibitors of cyclin-dependent kinases. *Trends Pharmacol Sci* 2002;23:417-425.
42. Faivre S, Djelloul S, Raymond E. New paradigms in anticancer therapy: targeting multiple signaling pathways with kinase inhibitors. *Semin Oncol* 2006;33:407-420.
43. Zimmermann GR, Lehar J, Keith CT. Multi-target therapeutics: when the whole is greater than the sum of the parts. *Drug Discov Today* 2007;12:34-42.
44. Weishaupt JH, Kussmaul L, Grotsch P, Heckel A, Rohde G, Romig H, Bahr M, et al. Inhibition of CDK5 is protective in necrotic and apoptotic paradigms of neuronal cell death and prevents mitochondrial dysfunction. *Mol Cell Neurosci* 2003;24:489-502.
45. Helal CJ, Kang Z, Lucas JC, Gant T, Ahlijanian MK, Schachter JB, Richter KE, et al. Potent and cellularly active 4-aminoimidazole inhibitors of cyclin-dependent kinase 5/p25 for the treatment of Alzheimer's disease. *Bioorg Med Chem Lett* 2009;19:5703-5707.
46. Kriegl L, Jung A, Engel J, Jackstadt R, Gerbes AL, Gallmeier E, Reiche JA, et al. Expression, cellular distribution, and prognostic relevance of TRAIL receptors in hepatocellular carcinoma. *Clin Cancer Res* 2010;16:5529-5538.

47. Nicoletti I, Migliorati G, Pagliacci MC, Grignani F, Riccardi C. A rapid and simple method for measuring thymocyte apoptosis by propidium iodide staining and flow cytometry. *J Immunol Methods* 1991;139:271-279.
48. Zhang J, Li H, Herrup K. Cdk5 nuclear localization is p27-dependent in nerve cells: implications for cell cycle suppression and caspase-3 activation. *J Biol Chem* 2010;285:14052-14061.
49. Eggers JP, Grandgenett PM, Collisson EC, Lewallen ME, Tremayne J, Singh PK, Swanson BJ, et al. Cyclin-dependent kinase 5 is amplified and overexpressed in pancreatic cancer and activated by mutant K-Ras. *Clin Cancer Res* 2011;17:6140-6150.
50. Liu JL, Wang XY, Huang BX, Zhu F, Zhang RG, Wu G. Expression of CDK5/p35 in resected patients with non-small cell lung cancer: relation to prognosis. *Med Oncol* 2011;28:673-678.
51. Poehlmann A, Roessner A. Importance of DNA damage checkpoints in the pathogenesis of human cancers. *Pathol Res Pract* 2010;206:591-601.
52. Cortez D, Wang Y, Qin J, Elledge SJ. Requirement of ATM-dependent phosphorylation of brca1 in the DNA damage response to double-strand breaks. *Science* 1999;286:1162-1166.
53. Zhao H, Piwnica-Worms H. ATR-mediated checkpoint pathways regulate phosphorylation and activation of human Chk1. *Mol Cell Biol* 2001;21:4129-4139.
54. Donzelli M, Draetta GF. Regulating mammalian checkpoints through Cdc25 inactivation. *EMBO Rep* 2003;4:671-677.
55. Tian B, Yang Q, Mao Z. Phosphorylation of ATM by Cdk5 mediates DNA damage signalling and regulates neuronal death. *Nat Cell Biol* 2009;11:211-218.
56. Yang Y, Mufson EJ, Herrup K. Neuronal cell death is preceded by cell cycle events at all stages of Alzheimer's disease. *J Neurosci* 2003;23:2557-2563.
57. Hoglinger GU, Breunig JJ, Depboylu C, Rouaux C, Michel PP, Alvarez-Fischer D, Boutillier AL, et al. The pRb/E2F cell-cycle pathway mediates cell death in Parkinson's disease. *Proc Natl Acad Sci U S A* 2007;104:3585-3590.
58. Turner NC, Lord CJ, Iorns E, Brough R, Swift S, Elliott R, Rayter S, et al. A synthetic lethal siRNA screen identifying genes mediating sensitivity to a PARP inhibitor. *EMBO J* 2008;27:1368-1377.
59. Courapied S, Sellier H, de Carne Trecesson S, Vigneron A, Bernard AC, Gamelin E, Barre B, et al. The cdk5 kinase regulates the STAT3 transcription factor to prevent DNA damage upon topoisomerase I inhibition. *J Biol Chem* 2010;285:26765-26778.
60. Barazzuol L, Jena R, Burnet NG, Meira LB, Jeynes JC, Kirkby KJ, Kirkby NF. Evaluation of poly (ADP-ribose) polymerase inhibitor ABT-888 combined with radiotherapy and temozolomide in glioblastoma. *Radiat Oncol* 2013;8:65.
61. Shelton JW, Waxweiler TV, Landry J, Gao H, Xu Y, Wang L, El-Rayes B, et al. In vitro and in vivo enhancement of chemoradiation using the oral PARP inhibitor ABT-888 in colorectal cancer cells. *Int J Radiat Oncol Biol Phys* 2013;86:469-476.
62. Hussain M, Carducci MA, Slovin S, Cetnar J, Qian J, McKeegan EM, Refici-Buhr M, et al. Targeting DNA repair with combination veliparib (ABT-888) and

- temozolomide in patients with metastatic castration-resistant prostate cancer. *Invest New Drugs* 2014.
63. Donawho CK, Luo Y, Luo Y, Penning TD, Bauch JL, Bouska JJ, Bontcheva-Diaz VD, et al. ABT-888, an orally active poly(ADP-ribose) polymerase inhibitor that potentiates DNA-damaging agents in preclinical tumor models. *Clin Cancer Res* 2007;13:2728-2737.
  64. Davidson D, Wang Y, Aloyz R, Panasci L. The PARP inhibitor ABT-888 synergizes irinotecan treatment of colon cancer cell lines. *Invest New Drugs* 2013;31:461-468.
  65. Asghar U, Meyer T. Are there opportunities for chemotherapy in the treatment of hepatocellular cancer? *J Hepatol* 2012;56:686-695.
  66. Qin S, Bai Y, Lim HY, Thongprasert S, Chao Y, Fan J, Yang TS, et al. Randomized, multicenter, open-label study of oxaliplatin plus fluorouracil/leucovorin versus doxorubicin as palliative chemotherapy in patients with advanced hepatocellular carcinoma from Asia. *J Clin Oncol* 2013;31:3501-3508.
  67. Yeo W, Mok TS, Zee B, Leung TW, Lai PB, Lau WY, Koh J, et al. A randomized phase III study of doxorubicin versus cisplatin/interferon alpha-2b/doxorubicin/fluorouracil (PIAF) combination chemotherapy for unresectable hepatocellular carcinoma. *J Natl Cancer Inst* 2005;97:1532-1538.
  68. Leung TW, Patt YZ, Lau WY, Ho SK, Yu SC, Chan AT, Mok TS, et al. Complete pathological remission is possible with systemic combination chemotherapy for inoperable hepatocellular carcinoma. *Clin Cancer Res* 1999;5:1676-1681.
  69. Douillard JY, Cunningham D, Roth AD, Navarro M, James RD, Karasek P, Jandik P, et al. Irinotecan combined with fluorouracil compared with fluorouracil alone as first-line treatment for metastatic colorectal cancer: a multicentre randomised trial. *Lancet* 2000;355:1041-1047.
  70. Ang C, O'Reilly EM, Carvajal RD, Capanu M, Gonen M, Doyle L, Ghossein R, et al. A Nonrandomized, Phase II Study of Sequential Irinotecan and Flavopiridol in Patients With Advanced Hepatocellular Carcinoma. *Gastrointest Cancer Res* 2012;5:185-189.
  71. Boige V, Taieb J, Hebbar M, Malka D, Debaere T, Hannoun L, Magherini E, et al. Irinotecan as first-line chemotherapy in patients with advanced hepatocellular carcinoma: a multicenter phase II study with dose adjustment according to baseline serum bilirubin level. *Eur J Cancer* 2006;42:456-459.
  72. Gornet JM, Azoulay D, Duclos-Vallee JC, Goldwasser F. Complete remission of unresectable hepatocellular carcinoma on healthy liver by the combination of aggressive surgery and high-dose-intensity chemotherapy by CPT-11. *Anticancer Drugs* 2000;11:649-652.
  73. Saltz LB, Cox JV, Blanke C, Rosen LS, Fehrenbacher L, Moore MJ, Maroun JA, et al. Irinotecan plus fluorouracil and leucovorin for metastatic colorectal cancer. Irinotecan Study Group. *N Engl J Med* 2000;343:905-914.
  74. Benson C, White J, De Bono J, O'Donnell A, Raynaud F, Cruickshank C, McGrath H, et al. A phase I trial of the selective oral cyclin-dependent kinase inhibitor seliciclib (CYC202; R-Roscovitine), administered twice daily for 7 days every 21 days. *Br J Cancer* 2007;96:29-37.

75. Wilhelm S, Carter C, Lynch M, Lowinger T, Dumas J, Smith RA, Schwartz B, et al. Discovery and development of sorafenib: a multikinase inhibitor for treating cancer. *Nat Rev Drug Discov* 2006;5:835-844.
76. Wilhelm SM, Carter C, Tang L, Wilkie D, McNabola A, Rong H, Chen C, et al. BAY 43-9006 exhibits broad spectrum oral antitumor activity and targets the RAF/MEK/ERK pathway and receptor tyrosine kinases involved in tumor progression and angiogenesis. *Cancer Res* 2004;64:7099-7109.
77. Fujimaki S, Matsuda Y, Wakai T, Sanpei A, Kubota M, Takamura M, Yamagiwa S, et al. Blockade of ataxia telangiectasia mutated sensitizes hepatoma cell lines to sorafenib by interfering with Akt signaling. *Cancer Lett* 2012;319:98-108.
78. Zhai B, Hu F, Jiang X, Xu J, Zhao D, Liu B, Pan S, et al. Inhibition of Akt Reverses the Acquired Resistance to Sorafenib by Switching Protective Autophagy to Autophagic Cell Death in Hepatocellular Carcinoma. *Mol Cancer Ther* 2014.
79. Zhai B, Sun XY. Mechanisms of resistance to sorafenib and the corresponding strategies in hepatocellular carcinoma. *World J Hepatol* 2013;5:345-352.
80. Demange L, Abdellah FN, Lozach O, Ferandin Y, Gresh N, Meijer L, Galons H. Potent inhibitors of CDK5 derived from roscovitine: synthesis, biological evaluation and molecular modelling. *Bioorg Med Chem Lett* 2013;23:125-131.
81. Weitensteiner SB, Liebl J, Krystof V, Havlicek L, Gucky T, Strnad M, Furst R, et al. Trisubstituted pyrazolopyrimidines as novel angiogenesis inhibitors. *PLoS One* 2013;8:e54607.
82. Liebl J, Krystof V, Vereb G, Takacs L, Strnad M, Pechan P, Havlicek L, et al. Anti-angiogenic effects of purine inhibitors of cyclin dependent kinases. *Angiogenesis* 2011;14:281-291.
83. Feldmann G, Mishra A, Bisht S, Karikari C, Garrido-Laguna I, Rasheed Z, Ottenhof NA, et al. Cyclin-dependent kinase inhibitor Dinaciclib (SCH727965) inhibits pancreatic cancer growth and progression in murine xenograft models. *Cancer Biol Ther* 2011;12:598-609.
84. Parry D, Guzi T, Shanahan F, Davis N, Prabhavalkar D, Wiswell D, Seghezzi W, et al. Dinaciclib (SCH 727965), a novel and potent cyclin-dependent kinase inhibitor. *Mol Cancer Ther* 2010;9:2344-2353.
85. Stephenson JJ, Nemunaitis J, Joy AA, Martin JC, Jou YM, Zhang D, Statkevich P, et al. Randomized phase 2 study of the cyclin-dependent kinase inhibitor dinaciclib (MK-7965) versus erlotinib in patients with non-small cell lung cancer. *Lung Cancer* 2014;83:219-223.
86. Corbel C, Wang Q, Bousserouel H, Hamdi A, Zhang B, Lozach O, Ferandin Y, et al. First BRET-based screening assay performed in budding yeast leads to the discovery of CDK5/p25 interaction inhibitors. *Biotechnol J* 2011;6:860-870.
87. Zhang B, Corbel C, Gueritte F, Couturier C, Bach S, Tan VB. An in silico approach for the discovery of CDK5/p25 interaction inhibitors. *Biotechnol J* 2011;6:871-881.
88. Kesavapany S, Zheng YL, Amin N, Pant HC. Peptides derived from Cdk5 activator p35, specifically inhibit deregulated activity of Cdk5. *Biotechnol J* 2007;2:978-987.
89. Zheng YL, Li BS, Amin ND, Albers W, Pant HC. A peptide derived from cyclin-dependent kinase activator (p35) specifically inhibits Cdk5 activity and phosphorylation of tau protein in transfected cells. *Eur J Biochem* 2002;269:4427-4434.

## **APPENDIX**

## 7 APPENDIX

### 7.1 Abbreviations

AEC	3-amino-9-ethylcarbazole
ANOVA	Analysis of variance between groups
APS	ammonium persulfate
ATM	ataxia telangiectasia mutated
ATP	adenosine-5'-triphosphate
ATR	ataxia telangiectasia and Rad3 related
BRCA1	breast cancer 1
BSA	bovine serum albumin
c-Abl	c-Abelson
cdc2	cell division cycle protein 2
Cdk	cyclin dependent kinase
Chk	checkpoint kinase
CIP	Cdk5 inhibitory peptide
CNS	central nervous system
CREB	cyclic adenosine monophosphate response element-binding
DMEM	Dulbecco's Modified Eagle Medium
DMSO	dimethyl sulfoxide
DNA	deoxyribonucleic acid
DSMZ	German Research Centre of Biological Material
DTT	dithiothreitol
ECL	enhanced chemiluminescence
EDTA	ethylenediaminetetraacetic acid
EGTA	ethylene glycol tetraacetic acid
ERK	extracellular signal-regulated kinases
FACS	fluorescence activated cell sorter
FCS	fetal calf serum
FL2-A	fluorescent channel 2 area
FL2-H	fluorescent channel 2 height
FS	fluorochrome solution

---

HCC	hepatocellular carcinoma
HEPES	4-(2-hydroxyethyl)-1-piperazineethanesulfonic acid
HRP	horseradish peroxidase
JCRB	Japanese Collection of Research Bioresources
MAPK	mitogen-activated protein kinase
min	minute
MOI	multiplicity of infection
PBS	phosphate buffered saline
PDGFR	platelet derived growth factor receptor
PI	propidium iodide
PI3K	phosphatidylinositol-4,5-bisphosphate 3-kinase
PMSF	phenylmethylsulfonyl fluoride
RFA	radiofrequency ablation
RNA	ribonucleic acid
rpm	revolutions per minute
SCID	severe combined immunodeficiency
SDS	sodium dodecyl sulfate
SDS-PAGE	sodium dodecyl sulfate polyacrylamide gel electrophoresis
SEM	standard error of the mean value
shRNA	short hairpin ribonucleic acid
siRNA	small interfering ribonucleic acid
TACE	transarterial chemoembolization
T/E	trypsin/EDTA
TEMED	<i>N, N, N', N'</i> tetramethylethylene diamine
TMA	tissue microarray
Tris	trishydroxymethylaminomethane
TUNEL	terminal deoxynucleotidyl transferase mediated deoxyuridine triphosphate Nick End Labeling
Tyr	tyrosine
VEGFR	vascular endothelial growth factor receptor

## 7.2 Publications

### 7.2.1 Original publications

Ehrlich SM, Liebl J, Ardelt MA, Mayr D, Kirchner T, de Toni E, Zahler S, Vollmar AM  
**Targeting cyclin dependent kinase 5 in hepatocellular carcinoma – a novel therapeutic approach.**

in preparation

### 7.2.2 Poster presentations

Stamm SM, Günther M, Mayr D, Kirchner T, Zahler S, Vollmar AM, Liebl J

**Cdk5 in HCC – a new therapeutic option.**

Deutsche Pharmazeutische Gesellschaft (DPhG) Jahrestagung 2013, October 9-11, Freiburg, Germany

Stamm SM, Günther M, Mayr D, Kirchner T, Vollmar AM, Zahler S, Liebl J

**Cyclin dependent kinase 5 as a promising target for hepatocellular carcinoma therapy.**

Interact – 6<sup>th</sup> Munich Life Science Symposium for Young Scientists, March 21-22, Munich, Germany

Stamm SM, Günther M, Mayr D, Kirchner T, Vollmar AM, Zahler S, Liebl J

**Cyclin dependent kinase 5 as a promising target for hepatocellular carcinoma therapy.**

SPSAS – Advances in Molecular Oncology: Translating Molecular Biology into Cancer Treatment 2013, February 3-8, São Paulo, Brazil

Stamm SM, Günther M, Mayr D, Kirchner T, Vollmar AM, Zahler S, Liebl J

**Cdk5: a novel target for treatment of HCC.**

Deutsche Pharmazeutische Gesellschaft (DPhG) Doktorandentagung 2012, November 14-17, Weimar, Germany

---

Stamm SM, Liebl J, Günther M, Mayr D, Kirchner T, De Toni E, Vollmar AM, Zahler S

**The Role of Cyclin Dependent Kinase 5 in Hepatocellular Carcinoma.**

Deutsche Gesellschaft für Verdauungs- und Stoffwechselkrankheiten (DGVS) Spring Conference 2011, May 27-28, Berlin, Germany (honored with the poster price)

### 7.3 Acknowledgements

An allererster Stelle möchte ich mich bei Frau Prof. Dr. Angelika Vollmar bedanken, dass Sie mir die Möglichkeit gegeben haben in Ihrer Arbeitsgruppe zu promovieren. Ich danke Ihnen ganz herzlich für die hervorragende fachliche und persönliche Betreuung, die produktiven Diskussionen und die hilfreichen Ratschläge. Vielen Dank, dass Sie sich immer Zeit für Ihre Mitarbeiter nehmen und sie Ihre Wertschätzung wissen lassen.

Zudem möchte ich Herrn Prof. Dr. Stefan Zahler danken, für die anregenden Diskussionen in unseren gemeinsamen Meetings und dass seine Tür nicht nur für technische Probleme immer offen steht.

Ein besonderes Dankeschön geht an meine wissenschaftliche Mentorin, Frau Dr. Johanna Liebl. Danke für deine Hilfe und Ratschläge, deine immerwährende Motivation und dass ich immer zu dir kommen konnte, egal mit welchen Anliegen.

Den Mitgliedern meines Prüfungskomitees gilt mein aufrichtiger Dank für Ihre Zeit und Mühe: Prof. Dr. Roland Kappler, Prof. Dr. Christian Wahl-Schott, Prof. Dr. Franz Paintner und Prof. Dr. Franz Bracher.

Ein großer Dank geht auch an unsere Kooperationspartner:

Herr Prof. Dr. med. Thomas Kirchner und Frau Prof. Dr. med. Doris Mayr von dem Pathologischen Institut der LMU München und Herr Dr. med. Enrico de Toni von der Medizinischen Klinik und Poliklinik II des Klinikums der Universität München in Großhadern für ihre Kooperation bei dem HCC Tissue Microarray. Herrn Dr. Michael Günther vom Lehrstuhl für Pharmazeutische Biologie und Biotechnologie, Department Pharmazie der LMU München für die Hilfe bei den HUH7 *in vivo* Versuchen.

Ein ganz besonders großes Dankeschön geht an alle aktuellen und ehemaligen Mitglieder der Arbeitsgruppe, für das super Arbeitsklima und die großartige Zeit im und außerhalb des Labors. Ich möchte Hanna, Bettina, Bianca, Jana, Ulla, Nina, Elisabeth, Sabine, Sebastian, Romina und Ruth danken, dass sie mich schon in meiner Masterarbeit herzlich aufgenommen haben und mich in den „wissenschaftlichen Alltag“ eingeführt haben.

Besonders Danken möchte ich auch meinen Kollegen, die parallel mit mir ihr Doktorarbeit angefangen haben, für die schönen gemeinsamen 3 Jahre: Michi, Verena, Simone, Flo, Lena und Tini.

Danke auch an meine Boxnachbarin Kerstin, für die vielen Gespräche über die Arbeit und über andere wichtige Dinge im Leben.

Ein großer Dank geht auch an Julia, für die Unterstützung an guten und schlechten Cdk5 Tagen. Ich hätte mir keine bessere Kollegin vorstellen können mit der ich nicht nur die Zellen und das Hotelzimmer in Sao Paulo geteilt habe.

Außerdem möchte ich mich bei Henri bedanken. Du hast die Hanna-Gruppe sehr bereichert. Und es ist immer gut einen Freund zu haben, der einen auch ohne Worte versteht. Henri, Julia und Lina, Danke auch für den Spaß, den wir außerhalb der Uni hatten und, dass ich dank euch jetzt viel fitter bin.

Ich möchte mich auch bei meinem Masteranden Max bedanken, für die riesige Hilfe im Labor und dafür, dass ich jetzt fast Fußball spielen kann.

Dani, Jessica und Bettina möchte ich danken für die kommunikativen Mittagessen. Und zusammen mit Steffi und Isabella für den lustigen Austausch außerhalb der Uni.

Ein großes Dankeschön gilt auch meiner Familie, die mir alles ermöglicht hat und mich immer unterstützt. Besonders möchte ich mich auch bei meinen Geschwistern bedanken, die wirklich immer und in jeder Lebenslage für mich da sind.

Mischa, ein riesen Dankeschön, dass ich mich immer auf dich verlassen kann, für deine nicht endende Motivation und dass ich dank dir auch an einem schlechten Tag glücklich bin.